REPORT DOCUMENTATION PAGE

Form Approved
OMB No. 0704-0188

1. REPORT DATE *(DD-MM-YYYY)*	2. REPORT TYPE	3. DATES COVERED *(From - To)*
12-09-2004	Final Report	03-18-2002- 09-30-2004

4. TITLE AND SUBTITLE
High Performance Electroactive Polymers for Naval Underwater Acoustic Applications

5a. CONTRACT NUMBER
N0001402-4-0418

5b. GRANT NUMBER

5c. PROGRAM ELEMENT NUMBER

6. AUTHOR(S)
Qiming Zhang

5d. PROJECT NUMBER

5e. TASK NUMBER

5f. WORK UNIT NUMBER

7. PERFORMING ORGANIZATION NAME(S) AND ADDRESS(ES)

8. PERFORMING ORGANIZATION REPORT NUMBER

9. SPONSORING/MONITORING AGENCY NAME(S) AND ADDRESS(ES)
Paul Armistead
ONR 331 Physical Science
Polymer Science Programs
800 N.Quincy St.
Arlington VA 22217

10. SPONSOR/MONITOR'S ACRONYM(S)

11. SPONSOR/MONITOR'S REPORT NUMBER(S)

12. DISTRIBUTION/AVAILABILITY STATEMENT
Approved for Public Release; distribution is Unlimited

13. SUPPLEMENTARY NOTES

14. ABSTRACT

Program objective was to develop electroactive polymers with performance superior than current materials for Navy transducers and electromechanical transduction (i.e. smart skins) applications. 3 approaches were proposed and 2 of them were investigated (the 3rd approach, which makes use of the polar-vector reorientation of liquid crystal polymers to generate high electromechanical efficiency, was not pursued due to funding limit). First, utilized the large strain associated with the molecular conformation change between different forms (polar and non-polar) to generate high electromechanical responses. New class of electroactive polymers, i. e. electrostrictive PVDF based polymers, have been developed and at the end of this program, a large quantity of the electrostrictive P(VDF-TrFE-CFE) terpolymer can be produced (~ 2 kg/batch), making it possible for the future prototype device development. Explored approach of using the delocalized electrons in organic materials to significantly raise the dielectric constant of polymeric materials; thus, polymeric materials with dielectric constant higher than 1,000 have been realized. Polymeric materials exhibit

15. SUBJECT TERMS
(balance of Abstract) electric field induced strain of higher than 10% with applied field at 25 V/•m.

16. SECURITY CLASSIFICATION OF:			17. LIMITATION OF ABSTRACT	18. NUMBER OF PAGES	19a. NAME OF RESPONSIBLE PERSON
a. REPORT	b. ABSTRACT	c. THIS PAGE			Qiming Zhang
UU	UU	UU	UU		19b. TELEPHONE NUMBER *(Include area code)* 814-863-8994

Standard Form 298 (Rev. 8/98)
Prescribed by ANSI Std. Z39.18

1-

High Performance Electroactive Polymers for Naval Underwater Acoustic Applications

March 2002 – September 2004

Final Program Report of
N00014-02-1-0418 P00001

Program Manager

Paul Armistead

ONR 331 Physical Sciences
Polymer Science Programs
800 N. Quincy St
Arlington, VA 22217

Submitted by

Qiming Zhang

187 Materials Research Laboratory
The Pennsylvania State University
University Park, PA 16802

Ph: 814-863-8994
Fax: 814-863-7846

December 2004

Technical Objectives

The overall objective of this program is to develop electroactive polymers with their performance much superior than the current materials for Navy transducers and electromechanical transduction (for example, smart skins) applications.

Technical Approach

In this program, three approaches were planed to be investigated:

(1) Making use of the large strain associated with the molecular conformation change between different forms (polar and non-polar) to generate high electromechanical responses (PVDF based electrostrictive polymers).
(2) All organic or polymer composites/fully functionalized polymers. In this approach, high dielectric constant organic filler and dielectric percolative phenomenon are exploited to produce polymeric-like materials with exceptionally high dielectric constant (>1,000). Consequently, high electromechanical response can be generated under a low driving electric field.
(3) Liquid crystal polymers where the polar-vector reorientation can generate high electromechanical efficiency, which has been demonstrated in this program that an electromechanical conversion efficiency of more than 75% has been obtained in this class of material. Due to limited resources in this program, this part work was not pursued actively in this program.

Accomplishments

The following is a brief summary of what have been achieved under the support of this program:

1. There are three areas of development of electrostrictive PVDF based polymers:

(1.1) Irradiated copolymers: optimized the processing conditions, especially developed a two step annealing process, for the film quality, the transverse electrostrictive strain, and coupling factor for the uniaxially stretched and high energy electron irradiated P(VDF-TrFE) copolymer. The irradiated electrostrictive P(VDF-TrFE) copolymer films exhibit an elastic modulus of 1 GPa, an electrostrictive strain of 4.5% under 90 MV/m, and a quasi-static electromechanical coupling factor k_{31} of 0.65 (under 90 MV/m AC signal). A two step annealing process was developed which makes it possible to have pin-hole free polymer films for the high energy electron irradiation.

(1.2) Terpolymers: systematically evaluated the dielectric and electromechanical properties of P(VDF-TrFE-CFE) terpolymers, as well as P(VDF-TrFE-CTFE) terpolymers. Carried out systematical study on the processing conditions, especially the annealing and mechanical stretching, on the elastic modulus, the field induced strain, and the elastic energy density of these terpolymers. Investigated the crystallization process in the P(VDF-TrFE-CFE) terpolymers which shows that CFE monomers are included in the crystalline phase. The terpolymer of P(VDF-TrFE-CFE) exhibits a dielectric constant of 50 (at 1 kHz), a thickness strain of -7%, and a transverse strain for uniaxially stretched films of 5% along the stretching

direction. The elastic modulus is 250 MPa for non-stretched films and 0.35 MPa for stretched films along the drawing direction.

(1.3) The scale-up of P(VDF-TrFE-CFE) terpolymers. With the support of this program, we were collaborating with Dr. F. Bauer at ISL of France in scaling up the production of the P(VDF-TrFE-CFE) terpolymers. A reactor with capability of synthesizing 2 kg/batch using the suspension method was developed at ISL. During the last two years, various synthesis conditions were investigated to reach the synthesis capability of 2 kg/batch. At Penn State, we supplied most of the TrFE monomers and characterized various properties of the terpolymer synthesized. Although it is still not reproducible, high quality P(VDF-TrFE-CFE) terpolymer can be produced in 2 kg batch size which makes it possible for any realistic prototype device development.

It is interesting to make a comparison of the electrostrictive PVDF polymers produced by the irradiation method and random terpolymer method. The terpolymer approach is attractive for large scale production of the electrostrictive polymer. The strain level of the terpolymer is higher. The irradiated copolymer shows higher elastic modulus (~1 GPa) and high electromechanical coupling factor. However, some of the defects introduced by the irradiation method is metastable and will be erased if the samples are heated to near melting temperature. For Navy transducers, the electrostrictive PVDF polymers may have too high a loss (>10%) for the operation at frequencies higher than a few kHz.

2. High dielectric composites and polymers with high electromechanical response. Four classes of composites were investigated and the material performance was improved progressively in the program.

(2.1) Electrostrictive PVDF matrix-Oligo CuPc dielectric composites. This is the first class of the high dielectric constant all-organic composite developed which shows that indeed with improved dielectric constant, electrostrictive strain can be induced with reduced field.

(2.2) Percolative composites in which conductive PANI was used as the filler to raise the dielectric constant of the terpolymer matrix. The composite exhibits a dielectric constant of higher than 1,000. A 10 times reduction in the applied field was achieved in inducing a strain of -2.7% with an elastic energy density of 0.17 J/cm^3. Furthermore, it was shown that the dielectric loss of the composites is actually the same as that of the terpolymer matrix which is important for the practical applications.

(2.3) Three component dielectric-percolative composites and fully functionalized polymers. The aim of this investigation is to show that the dielectric percolation can be used with insulating polymer matrix other than PVDF based electrostrictive polymers. In this approach, a high dielectric organic solid was used to raise the dielectric constant of the polymer matrix and this combined two phase matrix serves as the host for the conductive polymer guest to further increase the dielectric constant through the percolation. Indeed, a three component fully functionalized polymer exhibits a dielectric constant higher than 1,000, a thickness strain of 13% (under 27 MV/m) and a transverse strain of 7% (under 22 MV/m). The elastic energy density approaches 1 J/cm^3.

The work of the ultra-high dielectric constant polymers indicates that (1) delocalized electron system can be made use of to generate high dielectric response, (2) the nano-composites developed can exhibit dielectric loss even smaller than the matrix, (3) the high dielectric

response can maintain to high frequency (>1 MHz) in nano-composites. In these nano-structured polymers, it is important to prevent the formation of the percolation path among the delocalized electron fillers. The successful demonstration of this approach in this program opens up a new avenue to achieve high dielectric response, high mechanical response, in polymeric materials.

The following is a mode detailed account of the results from this program:

I. PVDF based electrostrictive polymers

1.1. High energy electron irradiated P(VDF-TrFE) copolymers

For PVDF based polymers, it is well known that the electromechanical responses can be influenced significantly by the polymer electroprocessing conditions. For the electron irradiated copolymers, we also found that the polymer processing conditions prior to the irradiation treatment can have very profound effects in the electromechanical properties of the polymer. Shown in figure 1 is the transverse strain for the uniaxially stretched P(VDF-TrFE) 68/32 copolymer films measured at room temperature and along the stretching direction. A strain of 4.5% can be induced under a field of 85 MV/m which is a quite large improvement compared with the response obtained in earlier samples (4% under 100 MV/m). The difference here is that in these new samples, a two step annealing process was used prior to the irradiation treatment, i.e., the stretched films were first annealed at a lower temperature (~120 °C) for a few hrs and then were followed by annealing at a higher temperature (134 °C, in this case) for 2 hrs. The initial purpose of introducing this two step annealing process is to improve the film mechanical quality. It was a pleasant side result that such a two step annealing process also brought about this improvement in the transverse strain response in the irradiated copolymer. Because of the reduction of the applied field to induce this high transverse strain, the transverse electromechanical coupling coefficient k_{31} was also improved, as shown in figure 1(b) where a k_{31} of 0.65 can be achieved. In fact, k_{31} obtained is even much higher than that in the piezoceramic PZT.

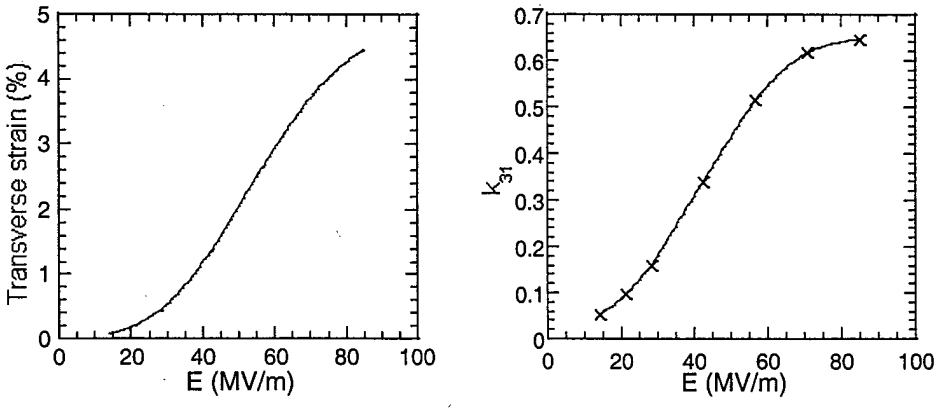

Figure 1.

1.2 P(VDF-TrFE) based terpolymers

In poly(vinylidene fluoride-trifluoroethylene) (P(VDF-TrFE)), it has been observed that the molecular conformation change between the all-trans and trans-gauche bonds is accompanied by a large strain (~10%). In the terpolymers of P(VDF-TrFE) with low level of chlorinated monomers, we showed that by a proper selection of the ter-monomer, a reversible change between the all-trans and trans-gauche bonds can be induced electrically, which, through the large ferroelastic coupling, results in a high electrostrictive strain (>-7%) and high elastic energy density ~1 J/cm^3. Shown in figure 2 is the dielectric constant and electric field induced thickness strain response of P(VDF-TrFE-CFE) terpolymer at 68/32/9 mol% composition and a thickness strain of more than -7% can be induced.

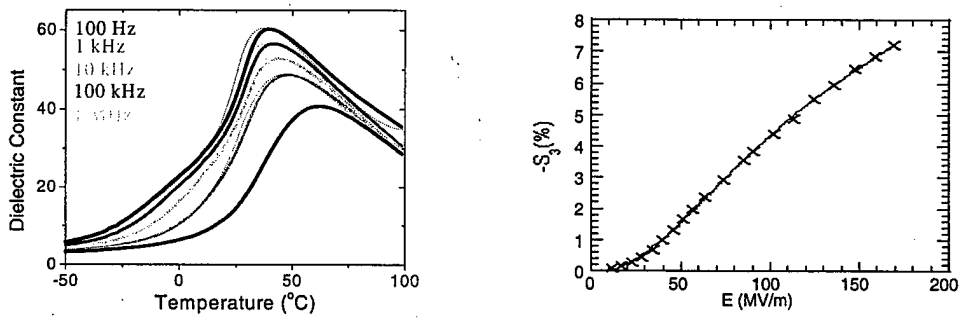

Figure 2. The dielectric constant and longitudinal strain of the terpolymer P(VDF-TrFE-CFE) 68/32/9 mol%

(1.2.1) Termonomor selections:

During the this program, several terpolymer samples which contain CTFE (CTFE: -CClF-CF_2-) termonomer synthesized by Mike Chung have been characterized. In addition, the terpolymer samples with C1F2E (-CClH-CFH-), also synthesized by Mike Chung, were evaluated. The results indicate that the field induced strain level and elastic energy density of these two classes of terpolymers are smaller that those obtained in the terpolymers with C1F1E (-CClF-CH_2-) as the termonomer, which seems to be consistent with the simple van der Wall radius consideration. (see Table I). As the bulkier termonoer is randomly introduced into the polymer chain, it will favor intra-chain all-trans conformation and interchain, TG and T_3G conformations. It is clear that the all-trans conformation is not desirable. Therefore, it is the termonoer that will have least tendency to induce intrachain all-trans conformation in the polymer crystalline lattice that should be used. Among the three termonors investigated, i.e., CTFE, C1F2E, and C1F1E, C1F1E is the one to produce the best electromechanical response and should be used. From this study, it may be further deduced that VCl (-CClH-CH2-) might be a better choice that C1F1E because it's overall size is even smaller than C1F1E.

Table I.

Composition	Strain (%)	Applied field	Elastic modulus (GPa)
CTFE 65/35/10	4%	150 MV/m	0.4
CTFE (MC292) 69/31/7.1	4.5%	200 MV/m	
C1F1E 62/38/4	4.5%	150 MV/m	1.1

C1F1E 68/32/9	7.2%	170 MV/m	0.3
C1F2E 70.6/29.4/3.6	4%	150 MV/m	0.47

(1.2.2) Improve the electromechanical response of the terpolymer P(VDF-TrFE-CFE)

In the past several years, several classes of terpolymers have been produced. Two synthesis methods were used to produce these terpolymers: the bulk method (M. Chung) and the suspension method (Q. Zhang). As shown in Table II, the terpolymers synthesized by the suspension method possess higher MW while the terpolymers synthesized by the bulk method show lower MW in comparison with the commercial copolymer.

Table II.

Sample	Composition	Mn	Mw	M_P	Polydispersity
Copolymer	65/35	86092	396580	264004	4.606
ISL-3 (suspension)	CFE 68/32/9	156302	506049	344676	3.237
ISL-4 (Suspension)	CFE 65/35/7	76021	702986	373169	9.247
MC289	CTFE 62.7/33.6/3.7	99735	790653	203929	7.927
MC292	CTFE 64.1/28.8/7.1 (69/31/7.1)	51470	242553	137402	4.712
Ter12	CFE 62/38/4	79704	243030	152607	3.049

(the terpolymers synthesized by the suspension method are indicated in the table)

For all the terpolymers synthesized except Ter12 (P(VDF-TrFE-CFE) 62/38/4 mol%), the elastic modulus is relatively low when compared with the irradiated copolymers. For the Ter12, the elastic modulus measured at room temperature is 1.1 GPa while for all the other terpolymers, the elastic modulus is low (see table I). Because of the low elastic modulus, the elastic energy density, even for ISL3 which exhibits a thickness strain of more than 7%, is below 0.75 J/cm^3. As a result, the electromechanical coupling factor for all the terpolymers (except the Ter12) is not very high (less than 0.4).

There are several issues which should be addressed in order to raise the electromechanical coupling factor in these terpolymers: (i) why the elastic modulus in these terpolymers is so low; (ii) what makes the Ter12 so different and possess much higher elastic modulus. The elastic modulus in the terpolymers will depend on the crystallinity and the morphology and size of the crystallites and polycrystallite-aggregates. Because the electromechanical response in the terpolymers is mainly from the crystalline region, raising the crystallinity will improve both the elastic modulus and field induced strain level. For instance, for the ISL3, if the strain level remains the same while raising the elastic modulus to 1 GPa, the elastic energy density will be increased to 2.5 J/cm^3, which is even much higher than that achieved in the single crystal PMN-PT (~ 1 J/cm^3) and will raise the electromechanical coupling factor significantly. Assuming a

dielectric constant of 50 and a field of 160 MV/m, the coupling factor k_{33} can be raised to 0.67. This example illustrates the importance of raising the elastic modulus for the terpolymers to achieve high elastic energy density and electromechanical coupling factor.

In the terpolymers, the termonomer will reduce the crystallinity in comparison with the corresponding copolymers. Therefore, it is important to keep the termonomor in the terpolymer to the minimum (Ter12 has a low CFE mol%), which is the amount just enough to convert the polymer into a relaxor ferroelectric with high electrostrictive strain. For a given termonomor, this minimum amount required will depend on the degree of the termonomor to be included in the crystalline region and the defects it creates in the crystalline lattice. For most practical polymer crystallization process, it is the crystallization kinetics that determines the concentration of the comonomer units to be included in the crystallites. For CFE based terpolymers, we have observed that by varying the crystallization temperature, the degree of CFEs to be included in the crystalline lattice can be changed, which will be discussed in the following sction. Furthermore, the experimental results indicate that CFE termonomors are included in the crystalline lattice which generates local lattice distortion.

(1.2.2.1) Effects of Crystallization Temperature T_x

By varying the crystallization temperature Tx, it was found that the fraction of polar and non-polar crystallites within the limits of the material can be varied. Crystallites formed during long times at the crystallization temperature T_x generally exhibit non-polar behavior. Crystallites formed during the rapid cooling process between T_x and room temperature generally exhibit more polar behavior. This is established most quantitatively by WAXD, and reinforced by FT-IR, polarization loop, and electromechanical strain measurements. DSC quantifies the fraction of crystallites formed at and below T_x, as well as the total crystallinity. Furthermore, as will be shown, crystallizing at higher T_x has an adverse effect on the electromechanical strain response and increases the polarization loop hysteresis.

i) DSC results

Figure 3 summarizes the DSC thermograms for the terpolymer crystallized from 112 to 142°C and then quenched to room temperature. As T_x increases, a melting peak at temperatures below T_x gradually appears. For the terpolymer samples with a T_x of 142 °C, the lower temperature melting peak ($T_m(1)$) is the major peak, indicating that most of the crystallites were formed during the rapid cooling process. In comparison, no such behavior was ever observed for the P(VDF-TrFE) copolymers: the CFE unit significantly slows the crystallization process and allows for the two crystallization peaks. The presence of CFE monomer in the VDF-TrFE polymer chains significantly lowers the crystallinity and crystal growth rate when compared with the copolymer. Table III lists values for the heats of fusion, melting temperatures, and crystallinity (X_c) for the terpolymer at various T_x compared against the copolymer at a similar composition ($T_m(1)$ is the lower temperature melting peak due to the crystallites formed during the rapid cooling and $T_m(2)$ is the melting from the crystallites formed at T_x).

Figure 4 provides the ΔH_m of the higher temperature melting peak (normalized to the total enthalpy, which thus can be regarded as the fraction of the crystallites formed at T_x to the total crystallites at room temperature) as a function of T_x. The data reveal that as T_x increases, this ratio decreases monotonically, reflecting the increased fraction of crystallites formed during the rapid cooling process.

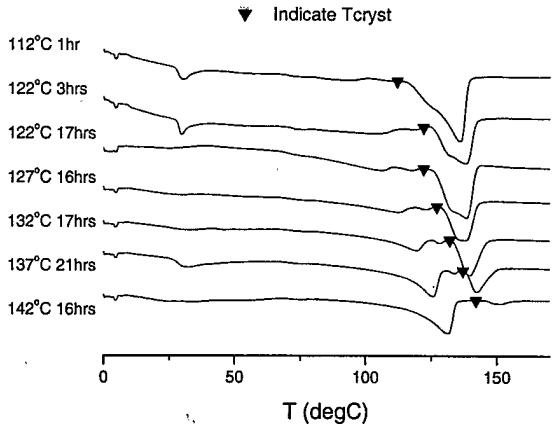

Figure 3. DSC traces for specimens with various crystallization temperatures (indicated in the figure).

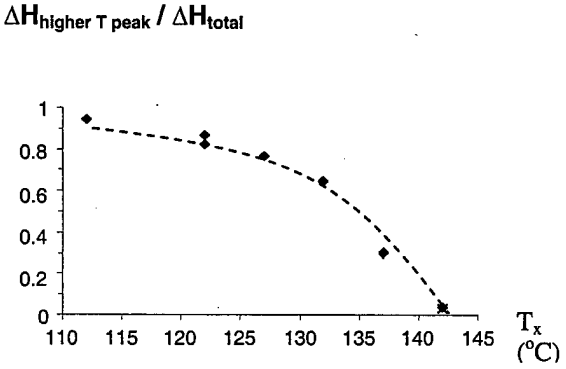

Figure 4.

Table III

Polymer	T_x (°C)	Cryst Time(hr)	ΔH (J/g)	$T_m(1)$ (°C)	$T_m(2)$ (°C)	X_C
Copolymer	140	16	31		158	80
Terpolymer	112	1	16.7		136.1	43
	122	3	18.0	103.2	138.1	46
	122	17	19.6	106.4	138.7	50
	127	16	19.5	112.3	137.5	50
	132	17	17.7	119.6	139.5	45
	137	21	19.5	125.9	142.9	50
	142	16	14.9	131.5	150.7	39

ii) Wide Angle X-ray Diffraction data

X-ray data were collected for the (110)/(200) reflection in order to interrogate interchain spacing and, through its breadth, crystalline order perpendicular to the chain direction. Also collected was the (001) reflection, whose breadth is characteristic of lattice continuity along the

polymer chain direction. For the (110)/(200) reflection, the data were acquired at selected temperatures between room temperature and T_x (taken on heating) to follow the evolution of the microstructure. For the (001) reflection, because of the limitation of the heating stage at the X-ray beamline, no measurements were taken at temperatures above 60 °C.

The X-ray data in the angle range of the (110)/(200) reflection acquired at room temperature are shown in figure 5(a). For the terpolymer films with T_x at 112 °C, 122 °C, and 127 °C, the X-ray data is relatively well-characterized by a single peak at $2\theta = 14.7°$, which represents the non-polar phase. The data fitting can be improved, however, by including a small peak at 15.3°, which is close to the position of the diffraction peak expected for the polar phase of the corresponding copolymer. As T_x is raised to 132 °C, this higher angle shoulder increases quite markedly and the best fitting to the data can be achieved by including two peaks, one near 15° and the other at 15.4° (two higher-angle peaks are seen most clearly in the 137°C scan). The phenomena of two polar peaks was examined and explained by Lovinger as the existence of both the planar-zigzag (all-trans) and 3/1 helix arrangements in the crystalline phase of P(VDF-TrFE) copolymers. The change in the diffraction patterns with increasing crystallization temperature can be seen in figure 5(b). In comparison with the X-ray data of the copolymer of similar composition, it can be deduced that the peak at lower angle ($2\theta = 14.7°$) is from the non-polar phase while the peaks at 15° and 15.4° indicate the gradual increase of the polar-phase component in the crystallites. Using the Scherer equation,

$$L_{hkl} = \frac{0.9\lambda}{B\cos(\theta)} \qquad (1)$$

the coherence of the crystal lattice perpendicular to a particular crystallographic plane can be deduced. In this equation, λ is the X-ray wavelength, B is the full width at half-maximum of the diffraction peak in question(in 2θ), and θ is the peak angular position. At room temperature, $L_{110/200} = 14$ nm for the non-polar phase.

The X-ray data for the (110)/(200) reflection acquired at 60 °C are shown in figure 6. At this temperature, the shoulder corresponding to the polar-phase has disappeared. At this temperature, the (110)/(200) peaks for the samples crystallized at different T_x are nearly identical in terms of both peak position and width. Although the peak position associated with diffraction from (110)/(200) of the non-polar phase does not show much change with temperature, the peak width is reduced (to below $B(2\theta) = 0.3°$) from that at room temperature, yielding $L_{110/200} = 23$ nm at 60 °C. One explanation for the observed increase in $L_{110/200}$ is that at room temperature, the non-polar and polar-phases coexist in the same crystallite, limiting the special coherence of the non-polar phase.

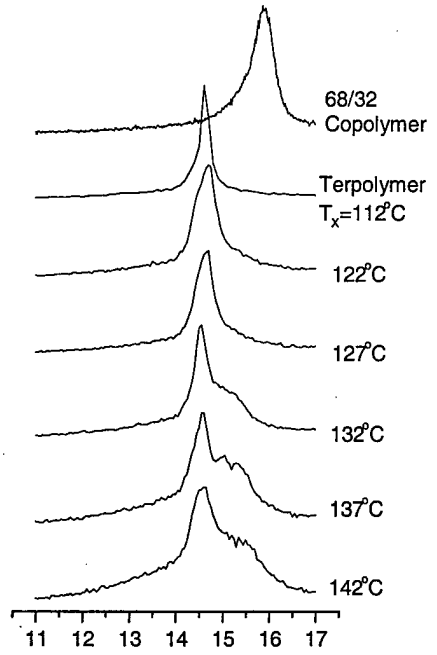

Figure 5.

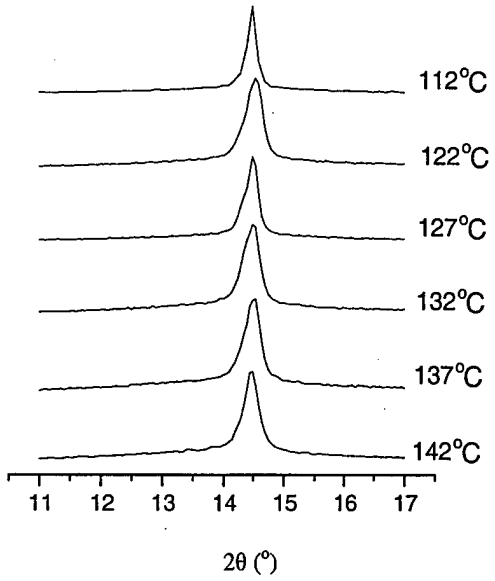

Figure 6.

It can be further deduced that in the same crystallite, there are regions with higher CFE fraction, which stabilizes the non-polar phase, and regions with lower CFE, which favor the polar-phase. The samples crystallized at higher T_x have more crystalline regions with lower CFE content (more exclusion of CFE from the crystallites) as reflected by the X-ray data. Such regions of relatively high and low CFE content are also suggested by FT-IR data.

X-ray data taken at $T = T_x$ for polymer samples with different T_x are shown in figure 7. At this temperature, the X-ray peaks arise from the diffraction of the crystallites with T_m higher than the original T_x. The (non-polar) peak position changes only slightly with temperature due to thermal expansion. On the other hand, there is a further reduction in the breadth of the (110)/(200) reflection to $B(2\theta) = 0.15^\circ$. Therefore, the coherent domain is now larger than 42 nm. These results indicate that $L_{110/200}$ for the crystallites formed during the rapid cooling process is at least twice as small as that formed at T_x. Furthermore, the crystallinity at the various T_x's evaluated by X-ray peak areas follows the same trend as determined by DSC, shown in figure 3.

The (001) reflections as a function of Tx are shown in figure 8; the peak positions are at the approximate location of the (001) reflection non-polar phase of the parent copolymer. For samples crystallized at different T_x, there is no indication of a (001) reflection from the polar phase, which is notably different than the data in the angular range of the (110)/(200) reflection. This suggests very small and defected polar domains along the chain direction. The broadness of the (001) peak indicates a very small coherent size along the polymer chain direction. Using the Scherer equation, it is deduced that the coherent X-ray scattering domain is about 1.5 nm, and is the same for all samples examined. Furthermore, even when heating the polymer samples to 60 °C, at which temperature the (110)/(200) reflection peak width decreases noticeably, there is no change in the (001) X-ray peak shape and width. Contrarily, the copolymer shows thick non-

polar domains, with L_{001} = 15 nm for the 68/32 copolymer. Thus, the presence of the chlorinated commoners induces nanodomains – in the stem direction, but not in the lateral direction.

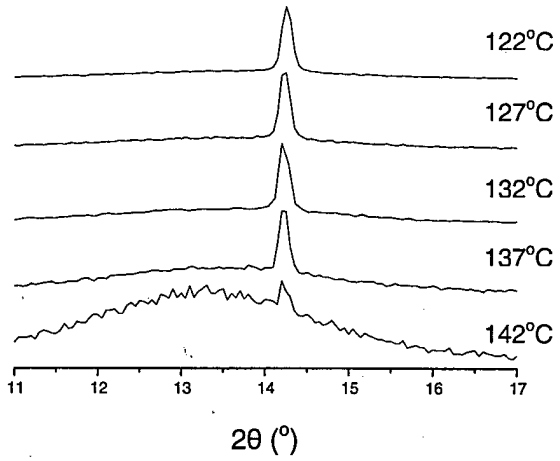

Figure 7.

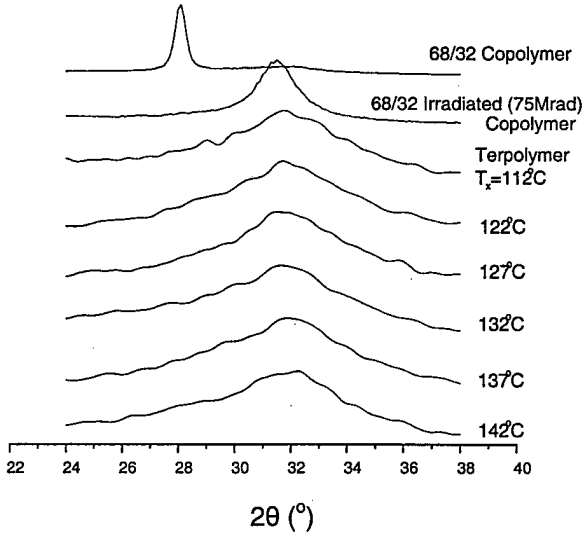

Figure 8.

iii) FT-IR results

In figure 9(d), the FT-IR data for the terpolymer samples with T_x at 112 °C and 142 °C are presented, which illustrate the change of the molecular conformations of the terpolymer samples with T_x (the copolymer is included for comparison). The absorbance peaks at 510 cm^{-1} (T_3G), 612 cm^{-1} (TG), and 1290 cm^{-1} ($T_{m>4}$) are chosen for analysis since they all represent motions of the CF_2 group to some extent. Figures 9(a), 9(b), and 9(c) give the conformation fractions for the 510 cm^{-1} (T_3G), 612 cm^{-1} (TG), and 1290 cm^{-1} ($T_{m>4}$) peaks, respectively.

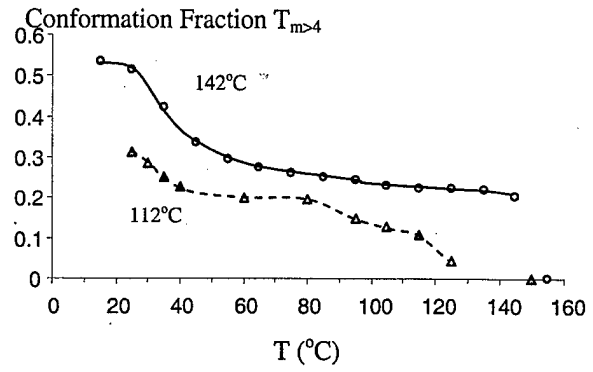
Conformation Fraction $T_{m>4}$
0.6
0.5
0.4
0.3
0.2
0.1
0
142°C
112°C
0 20 40 60 80 100 120 140 160
T (°C)

(a)

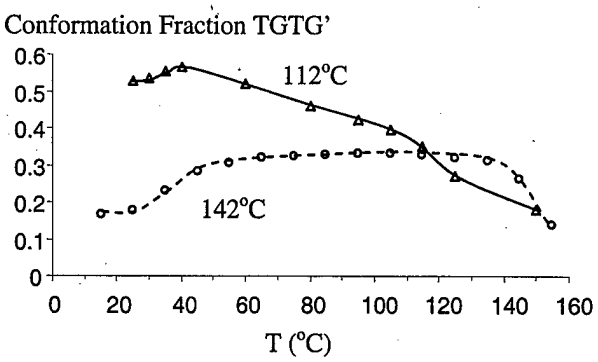
Conformation Fraction TGTG'
0.6
0.5
0.4
0.3
0.2
0.1
0
112°C
142°C
0 20 40 60 80 100 120 140 160
T (°C)

(b)

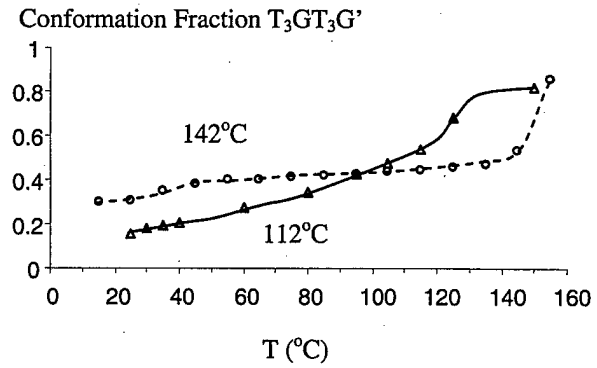
Conformation Fraction T_3GT_3G'
1
0.8
0.6
0.4
0.2
0
142°C
112°C
0 20 40 60 80 100 120 140 160
T (°C)

(c)

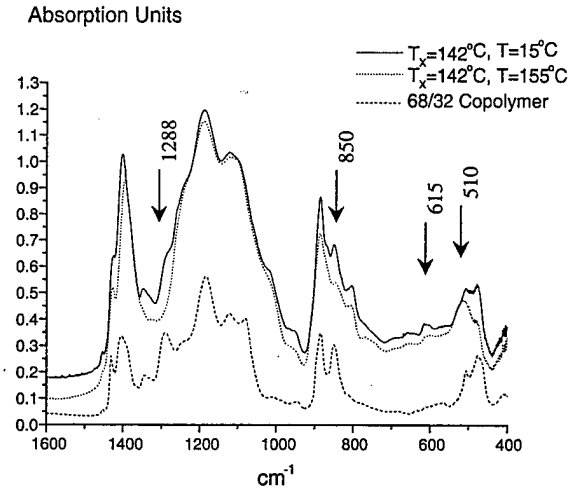

(d)

Figure 9.

Consistent with the X-ray data, at room temperature, the samples with T_x=142 °C show a higher fraction of the all-trans conformation. As the temperature is raised to 50 °C there is a drop in the all-trans conformation. The results indicate that there is a broad transition at temperatures near 40 °C, representative of a weak Curie transition. This transition temperature seems to be the same for all the samples with T_x ranging from 112 °C to 142 °C, although the transition is much weaker for samples with lower T_x, presumably due to the lower fraction of the polar regions in the polymers. The correlation between the size of the polar phase transition and the polymer composition again suggests that there are regions with higher CFE content (less polar) and regions with lower CFE content (more polar).

iv) Polarization hysteresis loop and electric field-induced strain data

The polarization hysteresis loops for the terpolymer samples crystallized at different T_x are shown in figure 10. A salient feature revealed by the data is the change of the polarization hysteresis for the terpolymer samples with different T_x. The terpolymer samples with lower T_x exhibit lower polarization hysteresis, i.e., a smaller P_r (remanent polarization) and E_c (coercive field). For example, the terpolymer films with T_x = 142 °C show an E_c of 20 MV/m, while for the sample with T_x = 112 °C, E_c = 11 MV/m.

Corresponding to this change in the ferroelectric behavior, the field-induced strain is also dependent on the T_x of the terpolymer samples. As shown in figure 11, the terpolymer sample with T_x at 112 °C exhibits a field-induced strain of -5.9% at 133 MV/m, while for the samples with T_x at 142 °C, the strain is reduced to -4.2% under the same field. This is too large of a change to be accounted for by crystallinity changes alone. The lower field-induced strain is due to already-existing ferroelectric domains that do not undergo the local conformation change upon application of the electric field.

These results indicate: (i) termonomer CFE reduces the crystallinity and crystallization rate; (ii) the crystallites formed at T_x have a higher inclusion of CFE compared with the crystallites formed during the rapid cooling, the amount crystallites formed at T_x reduces with T_x; (iii) the termonomers included in the crystallites generate defects which cause nano-domains along the polymer chain (~1.5 nm) (while the crystal lamellar thickness is ~15 nm); (iv) as a result, the

terpolymer samples with higher T_x exhibit larger polarization hysteresis and lower electrostrictive strain.

Further investigation will be carried out to improve the electromechanical response in these terpolymers, including the crystallization in supercritical CO2 as well as the crystallization under high pressure and temperature. The goal is to raise the crystallnity and increase the size of the polycrystallite aggregation so that the elastic modulus of the terpolymer can be raised markedly from the current level. The ultimate goal is to achieve high electromechanical coupling factor (>0.65) in the terpolymer under a reasonable DC bias field (<85 MV/m).

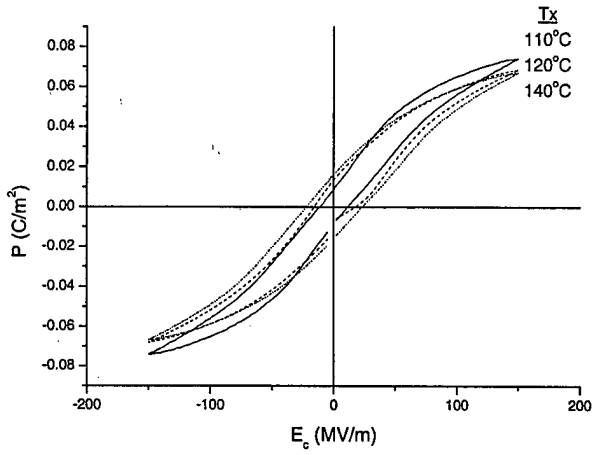

Figure 10.

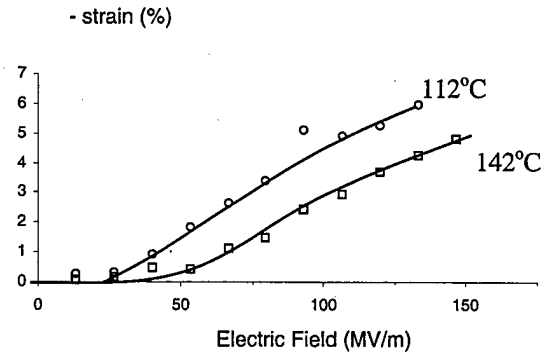

Figure 11.

(1.2.2.2) Effect of Annealing Temperature

Table IV summarizes the results of annealing temperature for cast-annealed (ca) and cast-stretched-annealed (csa) samples. Examination shows that csa samples exhibit a much larger remnant polarization P_r and a larger spontaneous polarization P_{sat} than the ca samples. Also, the heat of melting is generally higher, the modulus in the stretch direction is higher, and the electromechanical strain is lower in the stretched samples. This suggests the drawing process increases the total crystallinity of the system. Furthermore, the crystallites induced by casting, drawing, and annealing tend to have greater ferroelectric character than those simply formed by

casting and annealing. The increase in crystallinity results in a higher modulus of the bulk terpolymer.

Table IV. The effect of annealing temperature on properties. The data shown here is for a 65/35/8.6 mol% PVDF-TrFE-CFE terpolymer. The notations ca and csa mean cast-annealed and cast-stretched-annealed, respectively. All csa samples were stretched 5 to 6 times, and annealed for 5 hours. The Young's modulus was measured in the draw direction.

Processing Conditions	T_a (°C)	P_{sat} (mC/m^2) at 150 MV/m	P_r (mC/m^2) at 150 MV/m	H_m (J/g)	T_m (°C)	S_3 (%) at 100 MV/m	Young's Modulus (MPa)
ca	115	77	6.0	18	132	-3.4	320
csa	115	95	24.6	20	134	-2.5	N/A
ca	120	88	8.1	17	134	-3.3	160
csa	120	91	24.5	17	139	-3	480
ca	125	95	12.0	12	137	-3.3	170
csa	125	102	30.0	18	143	-2.9	350
Estimated E (±)	0.2	2	0.5	0.5	1	0.2	40

Annealing temperature also has a considerable effect on the measured properties. For this particular terpolymer composition, annealing at 115°C induces a high degree of crystallinity, whereas at 125°C crystallization is too slow to develop as high a degree of crystallinity. Note that the remanent polarization also increases with increasing T_a, which probably indicates that the improved kinetics for reorganization were able to anneal out some of the defects, thereby creating a more ferroelectric crystal structure. The increase in P_{sat} with increasing T_a is most likely due to the same effect.

(1.2.2.3) High Pressure Annealing

As has been reported in the literature, annealing at high pressures will shift the ferroelectric-paraelectric phase boundary to lower temperatures on the PVDF temperature-phase diagram and allow much higher crystallinities than achievable at atmospheric pressure annealed samples. However, for PVDF-TrFE with VDF ratios in the range of 0.6 to 0.82, T_C is below T_m, and the resulting effect of annealing at high pressures is relatively small.

Nonetheless, the effective T_m increases with pressure, which also allows crystallization and annealing to be done at much higher temperatures. Annealing at higher temperatures, by the Thomson-Gibbs equation, consequently allows a thicker lamellar thickness. And in most cases, thicker lamellae result in a higher crystallinity, since the amorphous region is used in the creation of the thicker lamellae. Thus, higher pressure allows higher crystallinity.

For the PVDF-TrFE-CFE terpolymer, our results show that slight increases in the degree of crystallinity can be obtained by annealing at high hydrostatic pressures. Table V illustrates this effect (an increase in ΔH_m from 22 J/g for the atmospheric pressure annealed to 25 J/g).

Table V. The melting point and heat of melting measured for samples annealed at high temperatures and pressures. This data is for the terpolymer of composition 0.65-0.35-0.086 PVDF-TrFE-CFE; all samples were cast, stretched (~5 times), and annealed.

T_a (°C)	Annealing Pressure (kpsi)	Annealing Time (hrs)	T_m (°C) (±0.5)	ΔH_m (J/g) (±0.5)
120	0	40	137	22
230	36.5	16	136	19

250	37	4	132	23
270	37	2	133	25

(1.2.2.4) Composition Optimization on Electromechanical Properties of P(VDF-TrFE-CFE)

We investigate the influence of the composition, especially the chlorofluoroethylen content, on the ferroelectric and electromechanical properties of the poly(vinylidene fluoride-trifluoroethylene- chlorofluoroethylene) (PVDF-TrFE-CFE). It was found that increasing the CFE from 0 to 9 mol% gradually converts the normal ferroelectric of the copolymer (in the compositions range of VDF/TrFE mole ratio between 64/36 to 75/25) to a relaxor ferroelectric, resulting in a nearly hysteresis free polarization loop and high electrostrictive response. On the other hand, increasing CFE content causes reduction in crystallinity, which will affect the elastic modulus and the induced polarization level of the polymer. These competing effects determine the desired terpolymer compositions for given applications. The electromechanical strain as a function of induced polarization and macro-polar phase fraction was modeled by a modified electrostrictive relation, which closely matches experimental data. It is found that the electrostrictive coefficient is relatively constant across the compositions investigated.

Presented in Figure 12 are the experimental results obtained for two compositions of P(VDF-TrFE-CFE). The composition of 65/35/8.6 mol% is a pure relaxor ferroelectric as can be concluded from the very low thermal hysteresis of the dielectric constant maximum, the X-ray diffraction (XRD) data showing only a single reflection representative of the non-polar phase in the (200)/(110) range, and the DSC data which exhibits only a melting endotherm and no detectable endotherm associated with the polar to non-polar phase transition. In contrast, the data for composition of 75/25/5.3 mol% display the presence of a polar phase, which is manifested in larger dielectric maximum hysteresis, a higher-angle reflection in the XRD data, and a DSC endotherm in the temperature range expected for the ferroelectric-paraelectric transition. The fraction of the polar phase X_F can be determined by the ratio of the polar phase peak area to the total crystalline peak area, as fitted from the (200/110) peaks of an XRD scan. Shown in Figure 13(a) is X_F thus determined as a function of CFE mol% for the terpolymers.

The PVDF-TrFE copolymer of the compositions studied here is

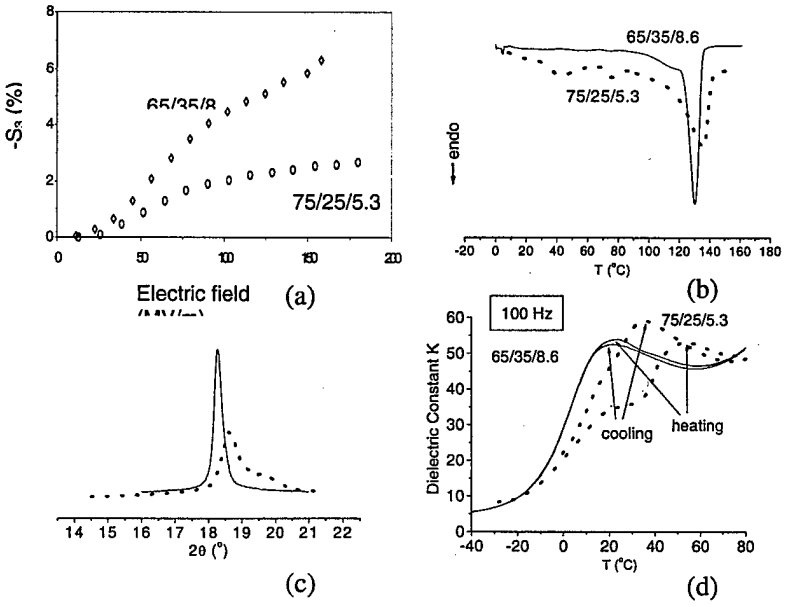

Figure 12. The (a) electromechanical longitudinal strain, (b) DSC trace, (c) WAXD data in the (200)/(110) range, and (d) dielectric constant K as a function of temperature for two compositions of PVDF-TrFE-CFE, 65/35/8.6 and 75/25/5.3. Note that for the terpolymer of 75/25/5.3, there is a lower temperature shoulder in the dielectric data taken during heating which is attributed to the coexisting relaxor phase.

primarily ferroelectric, where the ferroelectric-paraelectric transition is first order. Therefore, one measure of the presence of the polar-phase is the hysteresis of the dielectric constant maximum between the heating and cooling runs. Figure 13(b) shows this hysteresis as a function of CFE fraction. Also, the presence of the polar-phase can be measured by the DSC through the endothermic heat of transition ΔH_{Curie} associated with the polar to non-polar transition. This is shown in Figure 13(c). All data indicate that increasing the CFE fraction above 8.5% eliminates the polar crystalline regions.

Adding CFE units to the PVDF-TrFE, although inducing the change from ferroelectric to relaxor ferroelectric behavior, also has the adverse effect of reducing the crystallinity. As with copolymerization of most any two monomers, VDF and TrFE excluded, the crystallinity is expected to decrease sharply with increasing comonomer content. Thus, there is the careful balance of adding enough defects to the crystalline region to induce ferroelectric relaxor behavior, while meanwhile maintaining relatively high crystallinity to provide the electromechanical strain for which this system is designed. Figures 13(d) and 13(e) display the degree of crystallinity as determined by XRD and DSC and denoted as the degree of crystallinity X_C and the size of melting endotherm ΔH_m, respectively. X_C was determined by the ratio of the crystalline peak area (200)/(110) (which included both polar and non-polar reflections) to the sum of the areas of the crystalline peaks and the amorphous halo.

We will now discuss the relationship between the field-induced strain on other measurable polymer properties. Due to the existence of multiple phases within the terpolymer (polar crystalline regions, non-polar crystalline regions, and amorphous regions), there are four major possible origins of electromechanical strain within the terpolymer: electrostrictive strain, piezoelectric strain, ferroelectric domain wall motion, and Maxwell stress. Although electrostrictive strain exists for all phases, the dominating contribution is electrostriction in the non-polar region (the induced molecular conformation changes between the polar and non-polar phases, and nano-polar domain reorientation for regions initially oriented off-axis from the electric field are also described as electrostrictive).

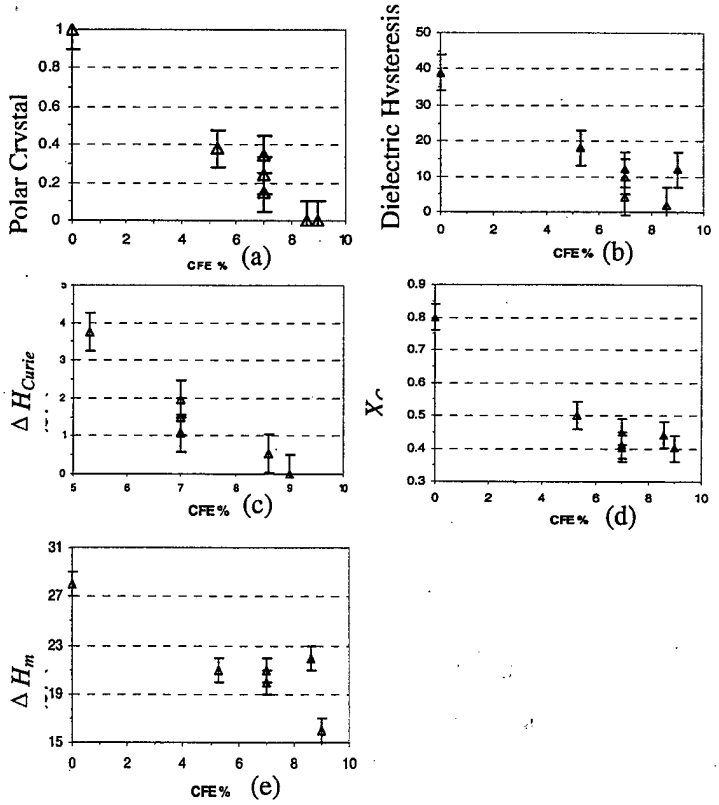

Figure 13. Plotted as a function of CFE composition: (a) polar crystal fraction X_F (area of the polar (200)/(110) peak divided by the total crystalline area), obtained by peak-fitting WAXD data; (b) dielectric hysteresis, determined by subtracting the cooling dielectric constant maximum from the heating dielectric constant maximum, measured at 100 Hz; (c) size of the 'Curie transition' endotherm, as determined by DSC; (d) degree of crystallinity X_C, determined by peak-fitting WAXD data; and (e) size of the heat of melting endotherm, determined by DSC.

Piezoelectric strain exists in the polar phase and involves dipole stretching. Ferroelectric domain walls propagating through the polar phase can accompany the polarization switching and lead to macroscopic strain. Maxwell stress-induced strain is caused by the capacitive force between the oppositely-charged surfaces of the sample. Earlier experimental results of PVDF-based polymers have shown that for PVDF-TrFE converted to a relaxor ferroelectric state, the electrostrictive strain is orders of magnitude larger than the others.

For an electrostrictive system with no external mechanical stress, the thickness strain S is related to the applied electric field E, induced polarization P, electric field-related electrostrictive coefficient M, and the charge-related electrostrictive coefficient Q by

$$S_3 = M_{33}E^2 = Q_{33}P^2 . \qquad (2)$$

where S is a second rank tensor, M, and Q are forth rank tensors, E and P are vectors. In Equation (2), a reduced matrix notation is used.

The data in Figure 13 show that the terpolymer has degrees of crystallinity between 0.4 and 0.5, and therefore the amorphous phase cannot be overlooked. The Young's modulus of unoriented, highly crystalline PVDF-TrFE is about 3 GPa; the Young's modulus of unoriented amorphous PVDF-TrFE is about 1 MPa; and the Young's modulus of our unoriented terpolymer varies between 200 and 500 MPa. Based on these moduli, a large amount of connectivity must exist between the crystalline regions.

Because the amorphous region has such a low modulus, and the crystalline phase has a high degree of interconnectivity, one can assume that the strain created from the crystalline regions is effectively transmitted to the bulk with little drag from the amorphous regions. Moreover, as noted by Furukawa, the contribution to the polarization comes almost exclusively from the crystalline regions. This allows us to write the bulk thickness strain as proportional to the square of the bulk polarization. There is one more factor that must be multiplied in, however: since the strain from the crystalline polar regions is very small compared to the strain from the non-polar regions, but the polar regions do have an considerable polarization, a factor counting the fraction of polar regions X_F must be removed from the polarization. We obtain

$$S_{bulk} = -Q_{bulk}[P_{bulk} \cdot (1 - X_F)]^2 \qquad (3)$$

where Q_{bulk} is the charge-related electrostrictive coefficient relating the bulk polarization to the bulk strain.

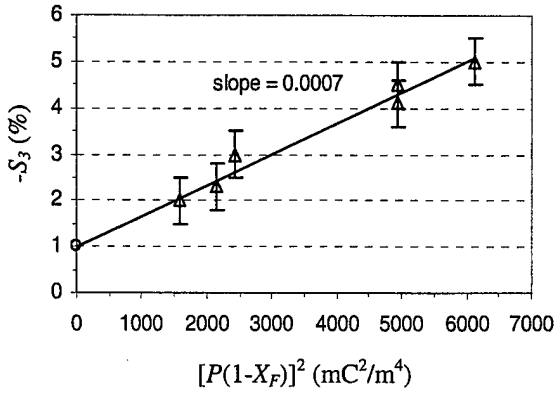

Figure 14. Plot of $[P(1-X_F)]^2$ versus strain. Each data point represents a different sample with a different composition. The slope of the linear-best fit is 7 m^4/C^2.

For terpolymers of low CFE content, the prevalence of the polar phase decreases the maximum strain level. For the copolymer without CFE, the strain level is quite low (~1% at 120MV/m). Using Equation 3, we can plot the thickness strain S_3 versus $[P(1-X_F)]^2$. The results are shown in Figure 14. Each data point represents a different sample with a different composition. P and S_3 were measured at an applied field of 120 MV/m, and X_F was taken from Figure 13(a). The charge-related electrostrictive coefficient Q_{bulk} obtained from the linear fit is 7 m^4/C^2. Note that in Figure 14, the fact that the data points closely follow the linear fit indicates that Q_{bulk}

is relatively constant across multiple PVDF-TrFE-CFE compositions. The highest S_3 obtained was -5% at 120MV/m for a composition of 65/35/8.6. Furthermore, decreasing the CFE fraction below ca. 8% causes an undesirable rise in the fraction of polar phase in the crystalline regions, leading to a reduction in the strain level. As the CFE mol% increases, however, the degree of crystallinity is adversely decreased. The experimental results indicate that the highest electrostrictive strain can be achieved in the composition of VDF/TrFE ratio of 70/30 mol% with 8 mol% of CFE. A thickness strain of more than -7% and a transverse strain in the stretched films of 5% can be induced with the elastic energy density approaching 1 J/cm^3.

(1.2.3) Dielectric study of the segmental relaxation in the terpolymers

One issue in the development of this class of electroactive polymers for Navy transducer applications is the dielectric loss. During this year, we investigated in some details on the origin of the dielectric relaxations of the terpolymers at near room temperature which could lead to strategies to modify the polymer to lower the dielectric loss. To provide better understanding of the relaxation processes in the terpolymers, we also investigated the dielectric relaxation of a copolymer with VDF/TrFE ratio similar to that of the terpolymer. As shown in Figure 15, near room temperature, there are actually two dielectric relaxations presence in the P(VDF-TrFE) 68/32 copolymer, one can be assigned as due to the defects in the crystalline region and the other was traditionally assigned as due to the glass transition in the amorphous phase (figure 4). However, study of the electric field poling effect on the copolymer indicates that both relaxation processes are affected by the electric field poling and relaxation strength is reduced after the poling. This result indicates that the dielectric relaxation which was assigned in the earlier studies as the glass transition in the amorphous phase in fact has very significant contribution from the crystalline phase. (The existence of the two relaxation peaks was also confirmed by the dynamic mechanical analysis).

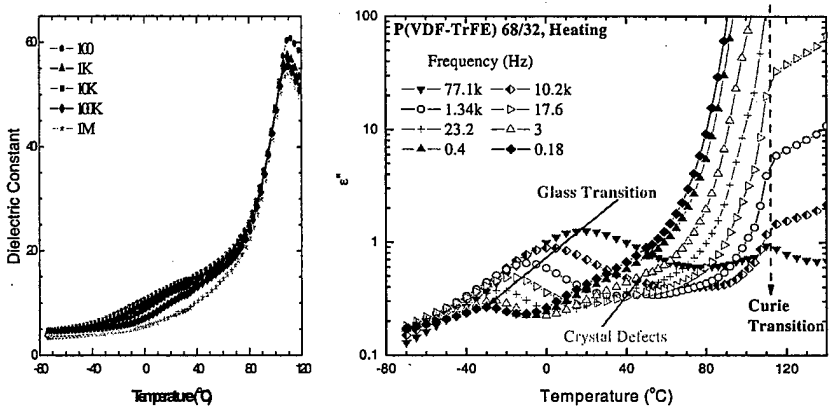

Figure 15

These two dielectric relaxations become stronger in the terpolymers (see Figure 16 for P(VDF-TrFE-CFE) 62.7/37.3/7.5

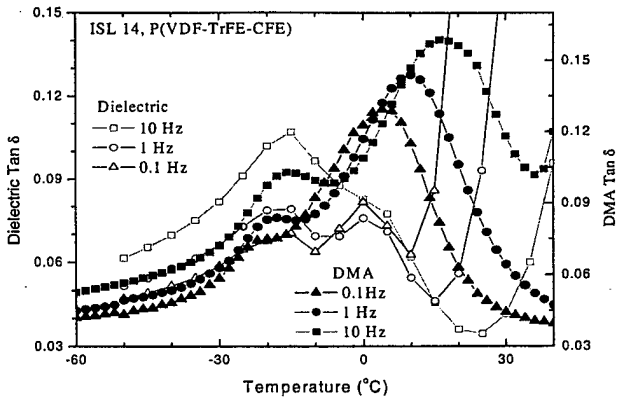

Figure 16

mol%), possibly due to increased defects in the crystalline region. In figure 16, the data from both the dielectric loss (open symbols) and mechanical loss (DMA, filled symbol symbols) are presented. The high (increased) dielectric loss at temperatures above 10 °C is due to the AC conduction which can be eliminated by improving the synthesis and polymer film processing conditions.

1.3 Scale-up of the P(VDF-TrFE-CFE) terpolymers

In collaboration with Dr. F. Bauer at Institute of St. Louis of France, relatively large batch of P(VDF-TrFE-CFE) can be produced. Several compositions of the terpolymers have been synthesized in 1 kg to 2 kg size. By adding a few parts, the reactor can be modified to produced 20 kg/batch (current size is 2 kg/batch).

II. Ultra-high dielectric constant composites and polymers

Besides the electrostrictive PVDF based polymers, we are also devoting efforts on raising the dielectric constant of polymeric materials by several orders of magnitude compared with the polymers currently in use. In this area, we are investigating the all-organic high dielectric constant composites which are flexible and possess elastic modulus very similar to the polymer matrix. The main purpose of this research and development effort is to develop a class of polymeric-like materials which can generate high strain (>10%) and high elastic energy density (~ 1 J/cm^3) with a low applied field (10 MV/m, this field level is similar to these used in the ceramic actuator materials).

2.1 An all-organic composite actuator material with oligo-CuPc in electrostrictive PVDF matrix

In spite of the fact that the electrostrictive terpolymers exhibit high electric field induced strain and high elastic energy density, they suffer the shortcoming of high operation field. By working with thin films (a few μm thick, for instance), the operating voltage can be reduced to several hundred volts, however, it will be advantageous to have a polymeric material which can be operated under low applied field directly. The basic reason for such high applied fields to generate high elastic energy density in the current terpolymers is the energy conservation. The stored elastic energy density when a polymer is strained is $U_S = ½ Y S^2$, where Y is the Young's modulus and S is the strain. For an electroactive material, the total elastic energy density from all the strains generated cannot exceed the input electric energy density because of the energy conservation. As a linear dielectric material, this input electric energy density from the external electric source is $U_E = ½ K\varepsilon_0 E^2$, where E is the applied field, ε_0 is the vacuum dielectric permittivity (=8.85x10^{-12} F/m), and K is the dielectric constant of the polymer. In most of the polymeric materials, the dielectric constant K is less than 10. Even for the electrostrictive PVDF based terpolymers, which possesses a dielectric constant around room temperature higher than 50 and is the highest among the known polymers, the dielectric constant is still far below those in the inorganic materials, many of which can reach more than 5,000. Therefore, in order to generate a high input electric energy density which can be converted to strain energy, a high electric field is required.

In order to raise the dielectric constant, we take the composite approach in which the electrostrictive PVDF based polymer as the matrix and the high dielectric constant organic solids as the filler. The dielectric constant >50 and electrostrictive strain >4% of the electrostrictive PVDF based polymer are highly desirable for the matrix material. In the past, it has been shown that in several semiconductor organic solids, a very high dielectric constant (>10^5) can be achieved. The high dielectric constant in these organic solids originates from the delocalized electrons in conjugated π-orbitals (eka-conjugate). In these organic molecular solids, the possible Jahn-Teller type effect can stabilize the orbital delocalization, which when coupled with high charge transport in these molecules such as the polaronic hopping can generate high polarization response. A very high dielectric constant can be obtained (the dielectric constant is higher than 1,000 up to 1 kHz). As shown in figure 17, for a composite with 40 wt% CuPc, the breakdown field currently is 13 V/μm and a strain near 2% can be induced (solid curve with crosses, measured at 1 Hz). In figure 18, the dielectric constant of the composite as a function of the applied field is also presented. The modulus of the composite is 0.75 GPa.

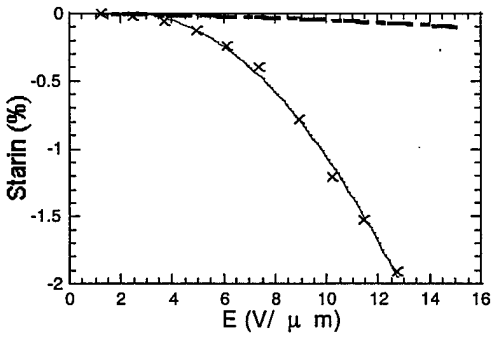

Figure 17. The thickness strain of the composite (the dashed line is from the polymer matrix)

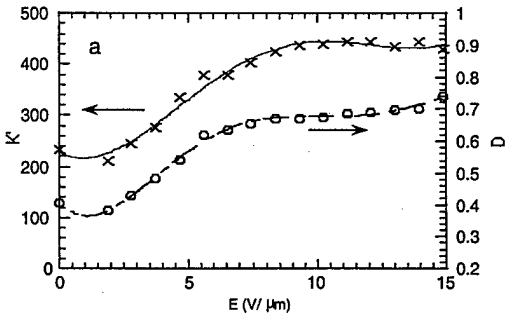

Figure 18. Dielectric properties as a function of the field

Under the assumption of the composites as homogeneous materials, the strain due to the Maxwell stress under a field of 13 V/μm is about -0.1%. For the electrostriction from the polymer matrix, it is also about -0.1%. The measured strain response, therefore, is about one order of magnitude higher than the combined strain from the two, assuming a uniform field distribution in the composite. One of the possible causes for such a high strain response is the large variations in the local fields in the composites which will enhance the strain response. In addition, bond length and conformation change in CuPc due to electron motions will also contribute to the strain response.

2.2. High dielectric constant polymers and composites—Percolative composites

Here, we investigate the approach using the conductive fillers to raise the dielectric constant. In a composite containing conductive particulates in an insulating matrix, when

the conductive phase concentration f is close to the percolation concentration f_c, a very high dielectric constant can be obtained:

$$\text{dielectric constant} = K_m (f_c - f)^{-q}$$

$$\text{conductivity} = \sigma_m (f_c - f)^{-q}$$

where K_m and σ_m are dielectric constant and conductivity of the matrix. q~1. therefore, a dielectric matrix with a high dielectric constant and low loss is preferred. Furthermore, the percolation theory predicts that the dielectric loss should not change with f, the concentration of the conductive filler when f<fc, and the dielectric loss is equal to that of the insulation matrix

In this investigation, we chose a conductive polymer, polyaniline (PANI), as the conductive filler, which has a relatively low elastic modulus (~2.3 GPa) in comparison to metal particles, whereby will not change the modulus of the composite very much from that of the polymer matrix. A poly(vinylidene fluoride-trifluoroethylene-chlorotrifluoroethylene) (P(VDF-TrFE-CTFE)) terpolymer at the composition of 62/26/12 mol% was selected as the matrix because of its relatively high room temperature dielectric constant (>50) and high electrostrictive strain. It will be shown that the dielectric constant for a composite containing 23 % in volume of PANI particulates can reach more than 2,000 (measured at 100 Hz), a more than 35 times increase from that of the matrix. More interestingly, a strain of 2.7% can be induced under a field of 17 MV/m, an near 10 times reduction in the field required for the same strain when compared with the polymer matrix, which by itself is a newly developed field type EAP exhibiting a high electromechanical response.

Polyaniline was synthesized using the conventional polymerization of aniline to produce fine emeraldine hydrochloride polymer particles. The product was extracted with ethanol to remove any unwanted impurities. The synthesized polyaniline was then coated with an insulating polymer to improve the breakdown field. Lauryl methacrylate, a long chain vinyl molecule, was chosen as the insulating monomer due to its good blend compatibility with the polymer matrix. The finely ground PANI powder was added to the degassed monomer and the reaction mixture was stirred by a magnetic stirrer and simultaneously shaken in an ultrasonic bath under a constant temperature of 60 °C. The final powder, having an average density of 1.3g/cm^3, was extracted with pentanol and dried. The average particle size of coated PANI (c-PANI), as determined by SEM image, is below 1 μm. Fourier transform infrared (FTIR) spectra indicated that the lauryl poly(methacrylate) has bonded chemically to the PANI backbone. Composite films were prepared using the solution cast method. P(VDF-TrFE-CTFE) terpolymer powder (the average density of 1.8g/cm^3) was dissolved in dimethylfomamide and then a proper amount of c-PANI powder was added to the solution. The solution was ultrasonically stirred to disperse the c-PANI powder.

(2.2.1) The dielectric response

Presented in figure 19 is the weak field dielectric property of the composites as a function of frequency, along with the data from the polymer matrix. The figure reveals several interesting features. At 100 Hz, the dielectric constant of a composite with only 25 % of c-PANI filler can reach more than 6,000. Considering the fact that at these compositions, the elastic properties of the composites are still very much the same as the polymer matrix and the dielectric loss is below 1, such a high dielectric constant for a polymeric-like material is quite impressive. Figure 20 summarizes the dielectric constant measured at 1 kHz as a function of the c-PANI volume % (both the dielectric constant and dielectric loss). As can be seen, the data can be fitted quite well by the dielectric percolation equation. The large increase in the dielectric loss at the

concentration f larger than 23% is caused by c-PANI aggregation and near percolation threshold. Therefore, the composites with the volume fraction f less than 23% were evaluated for the electromechanical responses.

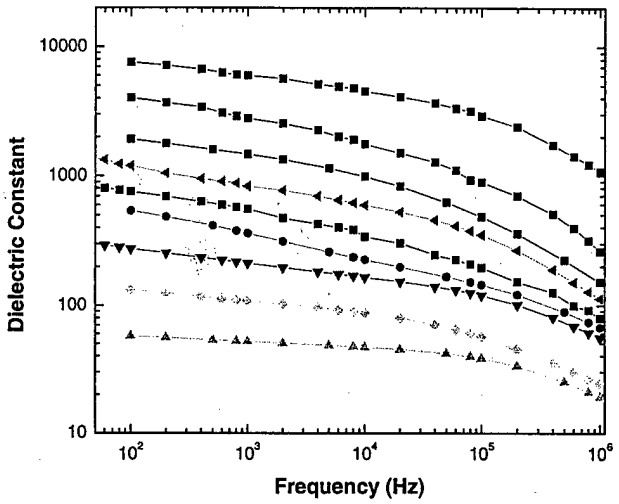

Figure 19. Dielectric constant of the percolative all polymer composites (from bottom to top: the c-PANI concentration increases from 0% to 25%)

The elastic modulus Y of the composites was measured at room temperature at the frequency of 1-2 Hz. The elastic modulus of the composite with 23 % c-PANI is 535 MPa. Compared with the elastic modulus of c-PANI fillers of 2.3GPa and the P(VDF-TrFE-CTFE) terpolymer of 400 MPa, the filler influences the elastic properties of the composite slightly and the composites remain very flexible. For the composites with 23 % c-PANI, the modulus is about 470 MPa.

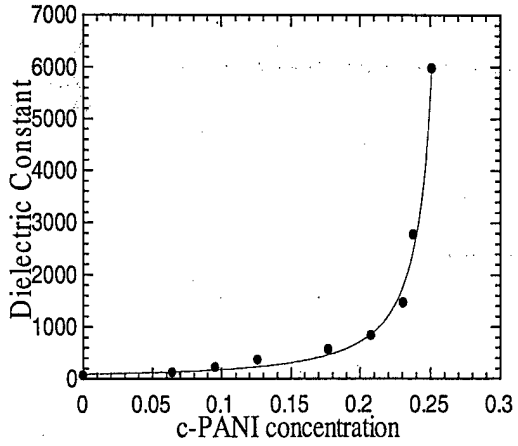

Figure 20. Dielectric constant measured at 1 kHz as a function of c-PANI volume concentration.

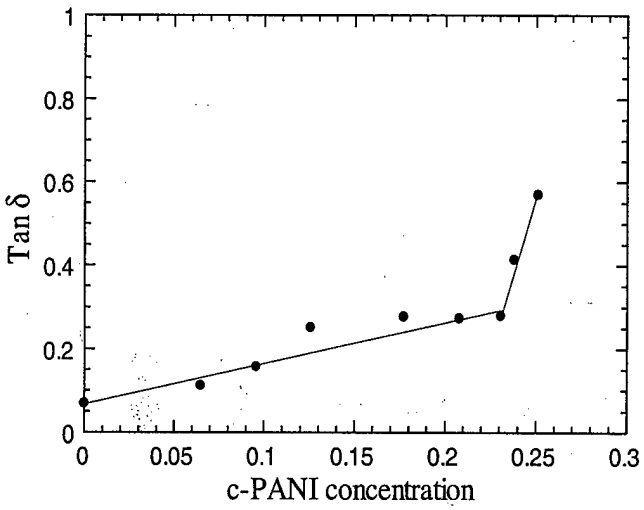

Figure 20

(2.2.2) The field induced strain response

The field induced strain was characterized at different applied fields at room temperature and under an AC field of 1 Hz. Presented in figure 21 is the strain amplitude measured versus the applied field amplitude for the composite containing different volume concentrations of c-PANI. A strain of -2.7% for the composite containing 23 % of c-PANI can be induced under a field of 17 MV/m. Combining the strain and elastic modulus yields the elastic energy density of 0.17 J/cm^3, which is larger than that of piezoceramics, for the composite under a field of 17 MV/m.

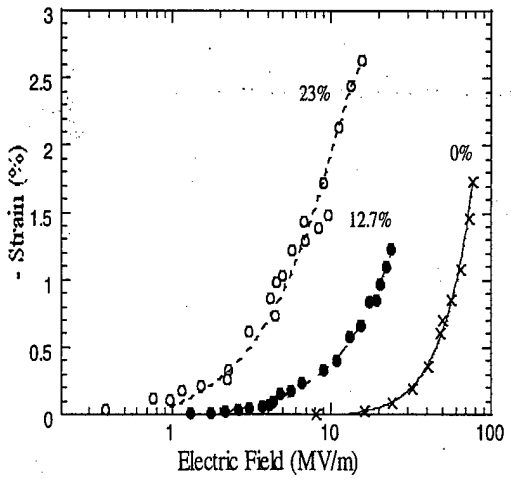

Figure 21.

The results of the strain measurement indicate that the field induced strain S is proportional to the square of the applied electric field, suggesting that the strain response originates from either the Maxwell stress (the electrostatic force), or the electrostriction, or both. For an isotropic dielectric material as the composites here, the strain induced by the Maxwell stress along the applied field direction is

$$S = \frac{1}{2} K\varepsilon_0 E^2 (1+2\nu)/Y. \qquad (4)$$

where ν is the Poisson's ratio. For the terpolymer matrix, early experimental results have shown that most of the strain response can be attributed to the electrostriction. For the composites with 12.7 % of c-PANI, figure 21 shows a strain of -1.25% induced under a field of 24 MV/m. With such a low c-PANI volume concentration, the average field in the terpolymer matrix should be nearly the same as 24 MV/m and as shown by the strain curve in figure 21, an induced strain in the pure terpolymer, which is used as the matrix for the composites, should be -0.075% under this field. Taking the data of the dielectric constant and elastic modulus, it can be estimated from eq. (4) that a Maxwell stress induced strain accounts for –0.87% thickness strain if a Poisson's ratio of 0.4 is assumed. The two strains combined accounts for more than 75% of the total observed strain response for the composite with 12.7 % of c-PANI. On the other hand, for the composite with 23 % of c-PANI, assuming a uniform field in the sample, there is very little electrostrictive strain from the terpolymer matrix under a field of 17 MV/m (see the curve in figure 2 measured from the terpolymer matrix). Therefore, measured strain response is three times of the combined strain responses (electrostriction and Maxwell stress effect) assuming a uniform field distribution in the film. The relatively low volume concentration (23 %) of c-PANI in the composite makes it unlikely that strain change in c-PANI is responsible for the observed strain response. Combining the data from the two composites suggest that as the filler concentration increases, the strain enhancement effect (the measured strain is much larger than the strain responses estimated assuming a uniform field distribution and no-interface effect) increases. When the c-PANI concentration increases, it is anticipated that the field distribution in the composites will become increasingly non-uniform and interface effects from the c-PANI-matrix interface will also become increasingly important, which may result in an enhanced electromechanical response. Such a strain enhancement effect has also been observed in other polymer systems with heterogeneous morphologies and has been demonstrated in a recent theoretical model.

(2.2.3) The dielectric loss of the composites

Figure 20 also shows that for the composites with c-PANI concentration higher than 10%, the dielectric loss is high. For the composites with f=0.23, the loss measured at 1 Hz at high fields is higher than 2 (D>2). For electromechanical applications, a low dielectric loss is needed. One question is whether the dielectric loss observed in these composites is intrinsic to the composite or it is due to some artificial effect in the composite caused by, for example, the agglomeration of the conductive fillers (or for the composites in 2.1, the agglomeration of Oligo-CuPc). To answer this question, we directly measured the strain-electric field hysteresis loop. If there is a high intrinsic dielectric loss, the strain hysteresis should also show a high hysteresis. Taking the electrostictive strain as an example, if the complex dielectric constant K possesses a large phase angle (a high dielectric loss), the strain-field relationship will exhibit a large hysteresis due to the lagging of the strain response to the applied field (see figure 22(c)). On the

other hand, if the high dielectric loss is caused by the conduction in the composites (as shown

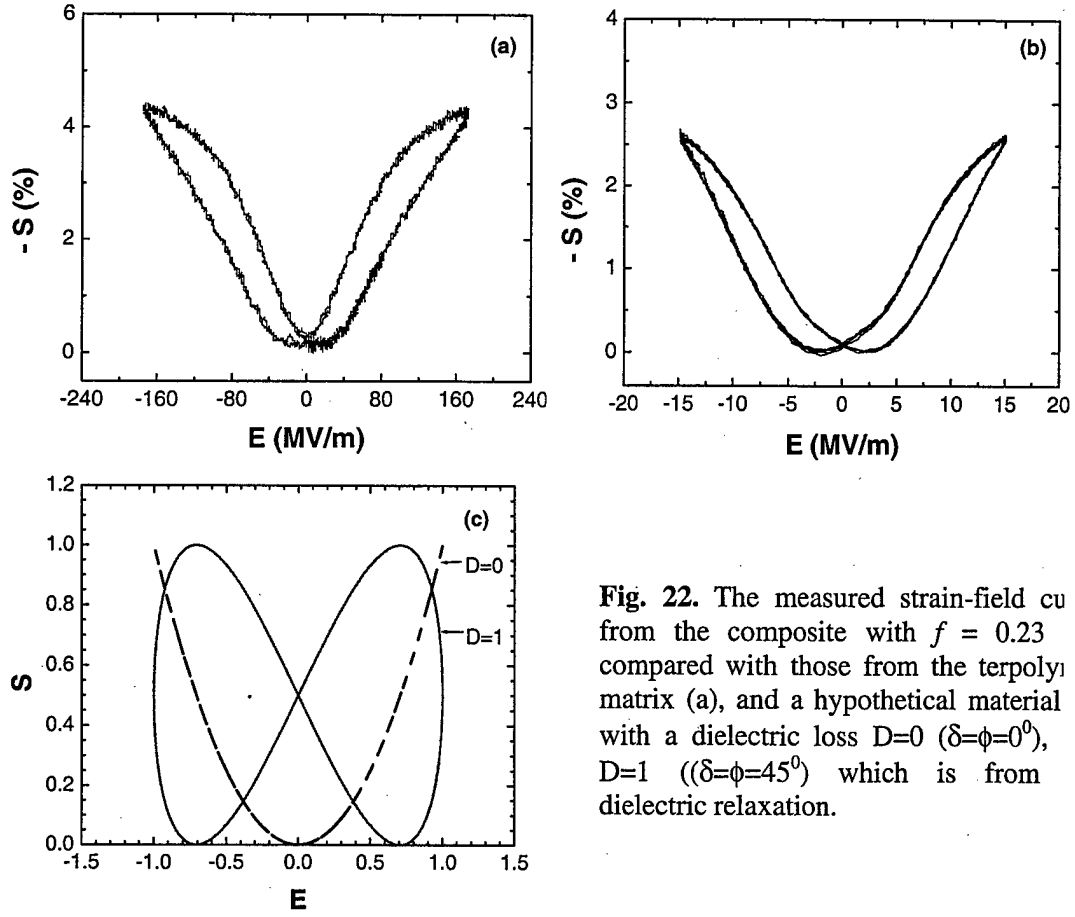

Fig. 22. The measured strain-field cu from the composite with f = 0.23 compared with those from the terpolyı matrix (a), and a hypothetical material with a dielectric loss D=0 ($\delta=\phi=0^0$), D=1 ($(\delta=\phi=45^0)$ which is from dielectric relaxation.

schematically in Figure 23) as likely to be the case for the composites investigated here, it will not affect the strain response and strain hysteresis. For the case shown in Figure 23, the total dielectric response of the combined material system is equal to the part ε_1^* from the capacitor component, which includes various dielectric contributions, and the part $j\sigma/\omega$ which is from the conduction through the resistor part, i.e.,

$$\varepsilon^* = \varepsilon_1^* - j\sigma/\omega \qquad (5)$$

and the dielectric constant used in the expressions for the electrostriction and Maxwell stress induced strain should be ε_1^* rather than ε^* where the symbol "*" indicates the complex dielectric constant. For the percolative composites, the loss part of ε_1^* should not be very much different from that of the polymer matrix for $f < f_c$.

Indeed, as shown in Figure 22(a) and 22(b) which compares the strain-field curve from the composite with f=0.23 to that from the terpolymer matrix, apparently, the two have very similar level of hysteresis, which is relatively small (corresponds to a dielectric loss D ~ 0.1). For further comparison, we show in Figure 22(c) the strain-field curve for a hypothetical electrostrictive material with a dielectric loss D=1 which is due to the dielectric relaxation. A very large strain hysteresis is observed. These results indicate that the intrinsic dielectric loss for these composites is not higher than the insulation polymer matrix.

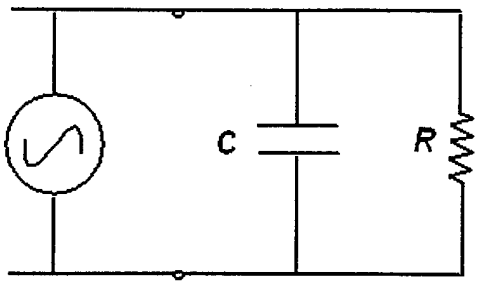

Fig. 23. An equivalent circuit for the composite near the percolation threshold where the presence of small amount of sub-phase which has compositions above the percolation forms parallel path (a resistor) with the majority phase which is still below the percolation (a capacitor), which illustrates the marked effect of the conductive minor sub-phase on the imaginary part of the dielectric constant and dielectric loss.

2.3 Fully functionalized dielectric-percolative three component nano-phase polymers

In the past, we have used composite approach in which high dielectric constant organic fillers and conductive polymers were physically blended with the matrix which has led to much improved electromechanical response. However, the composite approaches to form simple physical blends suffer from the adversely excessive agglomeration of the high-dielectric-constant organic and/or conductive polymer fillers due to incompatibility of these organic fillers with the polymer matrix, which increase the dielectric loss and reduce the breakdown field. From the application point of view, an ideal high dielectric constant polymers or composites should be mechanically robust and easy to process, i.e., the dispersibility of the fillers in the materials can be easily controlled. Obviously, chemically bonding the fillers to the backbones of the polymer matrix can improve the compatibility of the filler and matrix. Here we introduce a new approach in which high-dielectric-constant copper phthalocyanine oligomer and/or conductive polyaniline oligomer are chemically grafted to polyurethane backbones, and the resulting products-fully functionalized nano-phase polymers improve the compatibility of the two or three components, as well as offering good dielectric and mechanical properties and increasing the breakdown field. Consequently, these fully functionalized high-dielectric-constant nano-phase polymers exhibit high dielectric constant and electromechanical response.

It should also be pointed out that there is an added advantage of this fully functionalized nano-phase polymer approach. In a recent publication, Li has shown that the exchange coupling between the fillers and matrix with very large difference in the dielectric response can significantly enhance the dielectric response when the heterogeneity size of the composite is comparable to the exchange length. Indeed, we will demonstrate in this paper that with nano-size distributed fillers, the dielectric response of the fully functionalized nano-phase polymers is enhanced in comparison with the composites investigated earlier which have micron-size inclusions.

(2.3.1) Experimental

Materials Processing: The copper-phthalocyanine sheet oligomer (PolyCuPc) possessing peripheral carboxylic groups was synthesized by the solution method in high boiling-point solvent, nitrobenzene. The sample purity of copper-phthalocyanine tetramer (molecular formula, $C_{120}H_{40}N_{32}O_{32}Cu_4 \cdot 8H_2O$, and molecular weight, 2480) is 96.57%. The determined copper concentration in the tetramer is 6.08wt%, which reaches 82% of the theoretical value, 7.42wt%. The aniline oilgomer (PANI) capped with a phenyl group at one end and an amine at the other was synthesized by a general method in aqueous solution with oxidative coupling reactions. The

synthesized oligomeric aniline is a hexmer with a molecular formula, $C_{96}H_{82}N_{16}$ and molecular weight by GPC, 1486. Functionalized segmented polyurethanes (PU) with hydroxyl or

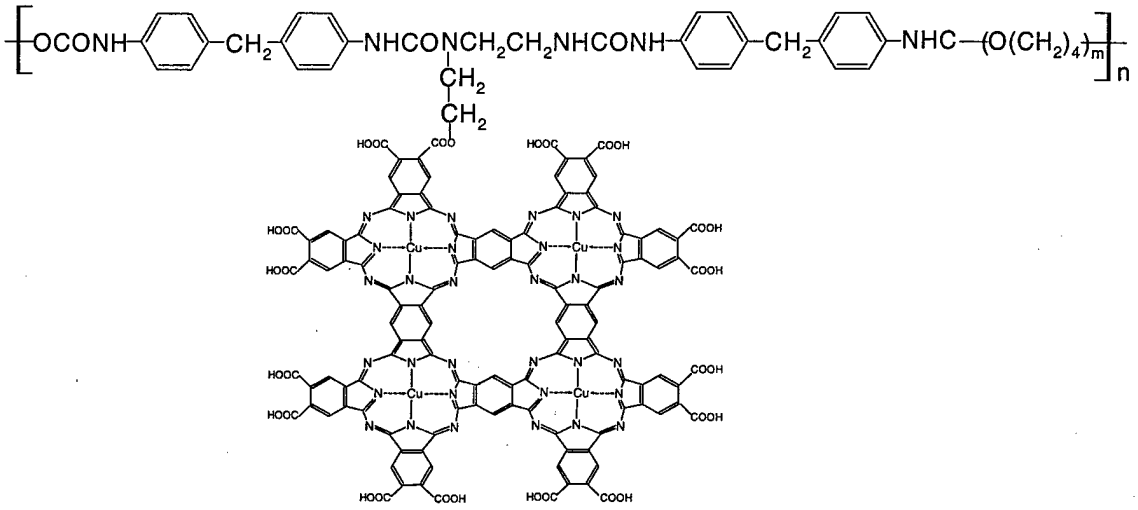

Figure 24 (a)

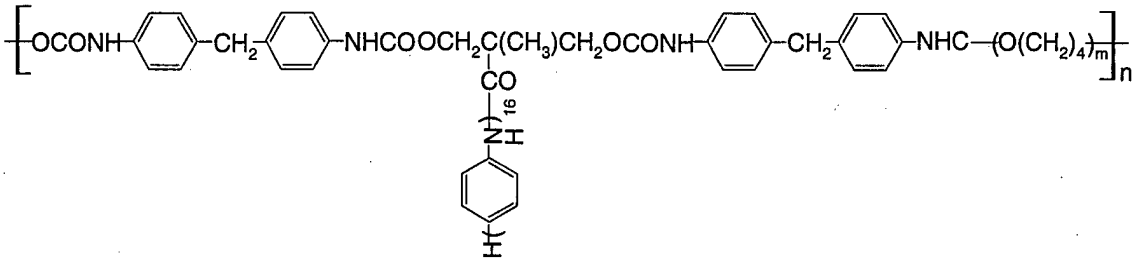

Figure 24 (b)

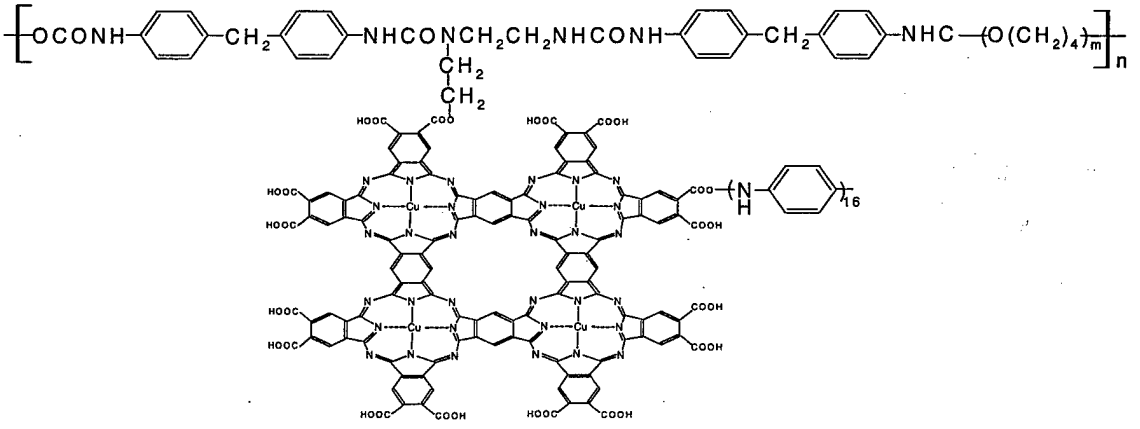

Figure 24 (c)

Figure 24. Schematic of chemical structures of oligomer graft polyurethanes: (a) CuPc oligomer (tetramer)-grafted PU (PolyCuPc-*g*-PU) (b) aniline oligomer (hexmer)-grafted PU (PANI-*g*-PU), and (c) PU grafted with CuPc oligomer (tetramer) and aniline oligomer (hexmer) (PANI-*g*-PolyCuPc-g-PU).

carboxylic side groups (PUOH and PUCOOH) were prepared by a typical two-step condensation reaction of 4,4'-methylenebis(phenyl isocyanine) (MDI), polytertramethylene glycol (PTMG) with molecular weight of 1000, and dibutyltin dilaurate catalyst, as well as the chain extender, *N*-(2-hydroxyethyl) ethylene diamine) (HEDA) or dimethylolpropionic acid (DMPA). The molar ratio of the components is about 2mol MDI/1mol PTMG/1 mol HEDA or 2mol MDI/1mol PTMG/1 mol DMPA. Hence, the hard segment is approximately 35% by weight in the sample to make sure the sequent polymers keep the necessary mechanical strength. Aniline oligomer-grafted PU, PANI-*g*-PU, as shown in Figure 24(b) was synthesized by covalently linking, via an amidation reaction, the terminal amine of oligomeric aniline (PANI hexmer) to free carboxylic side groups belonging to the repetitive unit of functionalized segmented polyurethane, PUCOOH. The initial weight ratio of the components is 15wt%PANI/85wt%PUCOOH , and analysis of the Soxhlet extracted sample determined 60% of the amidation degree (graft degree) for the PANI-*g*-PU sample. Similarly, CuPc oligomer-grafted PU, PolyCuPc-*g*-PU, as shown in Figure 6(a) was synthesized by covalently attaching, via an esterification reaction, the peripheral carboxylic groups of the copper-phthalocyanine sheet oligomer (PolyCuPc tetramer) to free hydroxyl side groups belonging to the repetitive unit of functionalized segmented polyurethane, PUOH. The initial weight ratio of the components is 30wt%PolyCuPc/70wt%PUOH, and analysis of the Soxhlet extracted sample determined 72% of the esterification degree (graft degree). PU grafted with CuPc oligomer (tetramer) and aniline oligomer (hexmer), PANI-*g*-PolyCuPc-*g*-PU, as shown in Figure 24(c) was synthesized simultaneously via both an amidation reaction between the terminal amine of oligomeric aniline (PANI hexmer) and the peripheral carboxylic groups of the copper-phthalocyanine sheet oligomer (PolyCuPc tetramer), and an esterification reaction between the peripheral carboxylic groups of the copper-phthalocyanine sheet oligomer (PolyCuPc tetramer) and free hydroxyl side groups belonging to the repetitive unit of functionalized segmented polyurethane, PUOH.

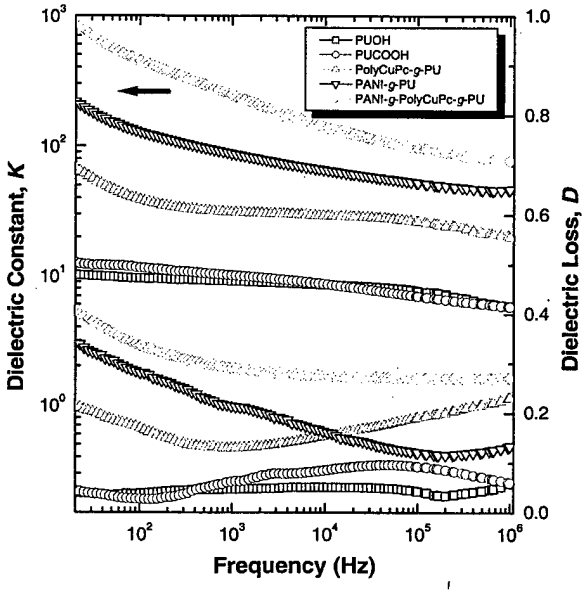

Figure 25. Dielectric constant *K* and dielectric loss *D* as a function of frequency ranging from 20Hz to 1MKz measured at room temperature for the oligomer grafted polyurethanes, PolyCuPc-*g*-PU, PANI-*g*-PU, and PANI-*g*-PolyCuPc-g-PU, compared with the polyurethane matrices, PUOH and PUCOOH.

The initial weight ratio of the components in the fully functionalized polymer is 15wt%PANI/25.5wt%PolyCuPc/59.5wt %PUOH, and the esterification degree of PolyCuPc and PUOH is about 65% and the amidation degree of polyaniline oligomer functionalized with CuPc oligomer is near 60%. The films were prepared from the in situ synthesized polymers using the solution cast method. The typical film thickness was about 40 μm.

(2.3.2) Results and discussion

Three oligomer graft polyurethanes as shown in Figure 24 were synthesized via graft post-reactions. Figure 25 shows the dielectric constant K and dielectric loss D as a function of frequency ranging from 20Hz to 1MHz measured at room temperature for both PU matrices and nano-phase polymers. The dielectric constant of the oligomer graft polyurethane is substantially increased compared with that of the PU matrices.

In these multi-component nano-composite polymers, the high dielectric constant of PolyCuPc enhances the dielectric constant of PU matrix while the conductive PANI raises the dielectric constant of the composite via the percolative phenomenon. Percolation theory predicts that the dielectric constant K_c of a composite consisting of conductive filler embedded in a dielectric matrix of dielectric constant K_m follows,

$$K_c = K_m\left(\frac{f_c - f}{f_c}\right)^{-q}$$

where f is the volume fraction of the conductive phase and f_c is the percolation threshold of conduction. In the three-component fully functionalized polymer, PANI-*g*-PolyCuPc-g-PU, PolyCuPC enhances the dielectric constant of the PU matrix. This combined two-component dielectric matrix serves as the high dielectric constant host for the percolative phenomenon, and a dielectric constant near 1000 is achieved at 20 Hz.

It is noted that dielectric constant of oligomer graft polymers is much higher than that of the simple physical polyurethane blends of two-components or three-components. For the comparison with the results earlier, we use the density of not grafted PolyCuPc (~ 1.6 g/cm^3), PANI (~ 1.3 g/cm^3), and PU (~ 1.13 g/cm^3) to estimate the volume content of each phase in the fully functionalized polymers here. At 20 Hz, PolyCuPc-g-PU with ca. 23 vol% of PolyCuPc can reach a dielectric constant of 60, which is even higher than the simple blend PolyCuPc-PU composites with 30 vol% of PolyCuPc which has a dielectric constant of 50. In contrast, the dielectric loss of the former is lower compared with the latter (D ~ 0.4 vs. D~0.6), which eliminates the possibility that the increased dielectric constant is due to the agglomeration. In the PANI-g-PolyCuPc-g-PU with ca. 14.4 vol% of PANI, the dielectric constant is 900 at 20 Hz while the three component blends with similar PANI concentration exhibit a dielectric constant of 160 at

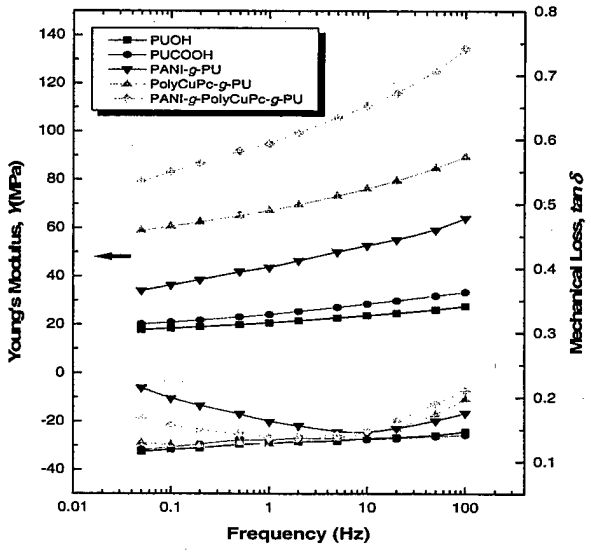

Figure 26. Young's modulus Y and mechanical loss $tan\delta$ vs frequency measured at room temperature for the oligomer grafted polyurethanes, PolyCuPc-*g*-PU, PANI-*g*-PU, and PANI-*g*-PolyCuPc-g-PU, compared with the polyurethane matrices, PUOH and PUCOOH.

the same frequency. The dielectric loss is nearly the same for the two (D~0.4). This enhanced dielectric response in oligomer graft polyurethanes here could be attributed to the much reduced filler size which enhances the exchange coupling (an interface effect) as theoretically predicted by Li.

The elastic modulus for these oligomer graft polyurethanes are presented in Figure 26. The elastic modulus of these graft polyurethanes increases due to the higher modulus of the

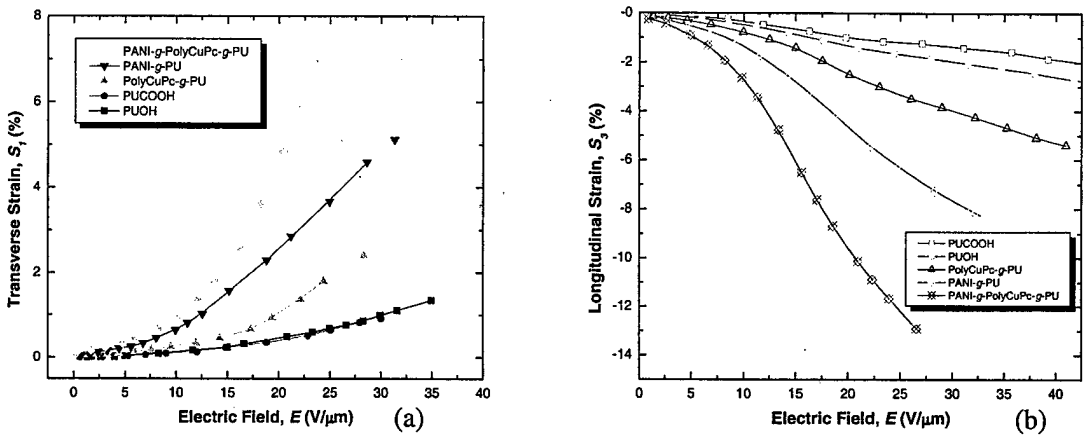

Figure 27. **(a)** The transverse strain S_1 as a function of the applied electric field E measured at room temperature for the oligomer graft polyurethane film. Curves from the top to bottom are for the samples: PANI-*g*-PolyCuPc-*g*-PU, PANI-*g*-PU, PolyCuPc-*g*-PU, PUCOOH, and PUOH. **(b)** The longitudinal strain S_3 as a function of the applied electric field E measured at room temperature for the oligomer graft polyurethanes. Curves from the top to bottom are for the samples: PUCOOH, PUOH, PolyCuPc-*g*-PU, PANI-*g*-PU, and PANI-*g*-PolyCuPc-*g*-PU. The applied-field frequency is 1 Hz.

nano-phase inclusions. The elastic modulus of the PANI-*g*-PolyCuPc-PU polymer (which has about 34 vol% of the total inclusions) reaches 100 MPa (at 1 Hz) (the PU matrix has a modulus at about 20 MPa). This value seems to be lower than that in the composites formed by physical blend, which is likely caused by the nano-phase inclusions and improved dispersion.

The electric field induced strain responses for these fully functionalized polyurethanes were characterized. Figure 27(a) presents the transverse strain response as a function of the applied field. Under a field of 23 V/μm, a transverse strain of 7% can be induced for the three-component fully functionalized polyurethane, which is quite high compared with other electroactive polymers. The thickness strain S_3 is presented in Figure 27(b), showing a -13 % strain induced under 27 V/μm. Although this is a quite high strain value under 27 V/μm field, it is lower than what expected from the results of Figure 27(a). For an isotropic material as studied here, the available experimental results as well as simple modeling results indicate that the thickness strain value $|S_3|$ should be larger than or at least equal to $2|S_1|$, which means that under a field of 23 V/μm, a thickness strain should be higher than -14% (the value in Figure 27(b) is less than -12%) for the three-component fully functionalized polyurethane. When extrapolated to 27 V/μm, data in Figure 27(b) suggest a thickness strain higher than -15%. This difference is caused by the mechanical clamping of Au electrodes, which possess an elastic modulus higher than 50 GPa, for the samples used in the thickness strain measurement. In the transverse strain measurement, the conductive carbon grease used should pose very little mechanical constraints

to the samples as has been shown in many other experiments. Such a mechanical clamping effect due to stiff electrodes will be more severe for polymers with lower elastic modulus. Indeed, for PU matrices which have elastic modulus of 20 MPa (1 Hz), the measured thickness strain is not much higher than the transverse strain.

Combining the strain and the elastic modulus for this polymer yields an elastic energy density of higher than 1 J/cm^3 for the thickness strain and 0.245 J/cm^3 for the transverse strain under 23 V/μm field. In comparison with the polyurethane matrix, the fully functionalized polymers presents more than ten times increase in the strain response and more than five hundred times increase in the elastic energy density. Compared with the three-component dielectric-percolative composite containing PolyCuPc and conductive PANI previously studied, higher breakdown field was observed in these graft polyurethanes.

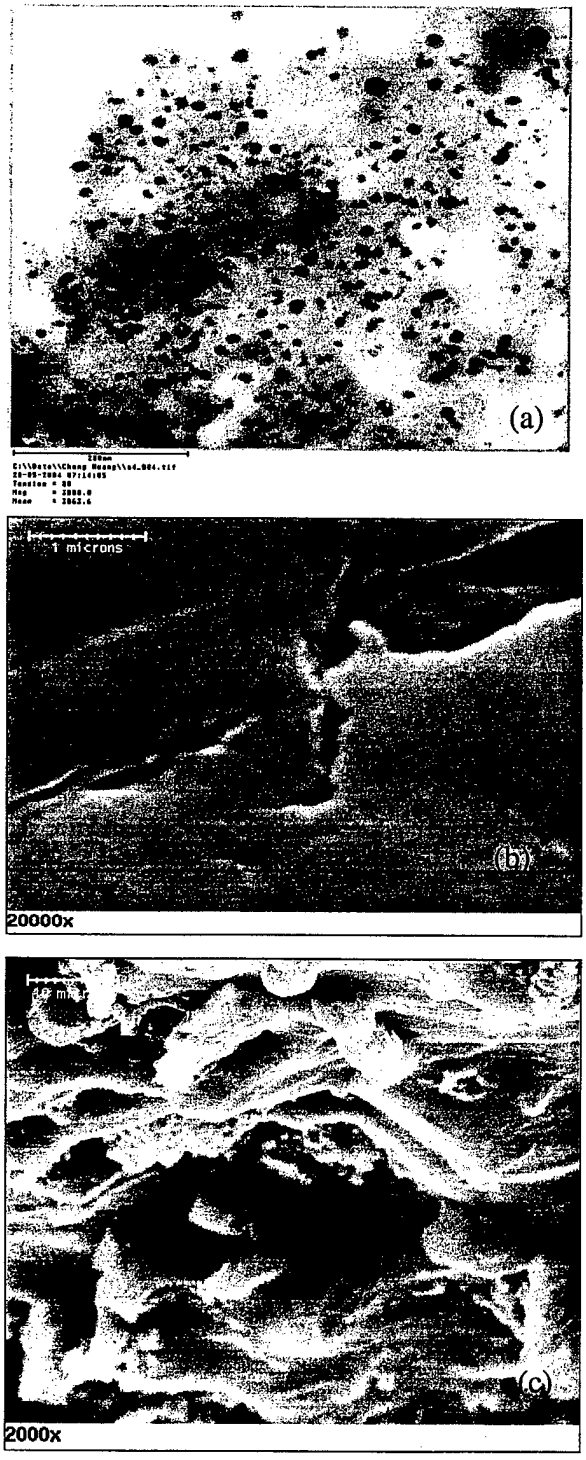

Figure 28. TEM micrograph of (a) PANI-*g*-PolyCuPc-*g*-PU, and SEM micrographs of (b) PANI-*g*-PolyCuPc-*g*-PU and (c) PANI/PolyCuPc/PU blend

The detailed microstructures of the fully functionalized polymers are investigated. The morphologies of the graft polyurethanes were detected by TEM and SEM. Figure 28(a) is the TEM micrograph for PANI-*g*-PolyCuPc-*g*-PU sample. Nano-phases with the near spherical shapes were formed in the polymer matrix. The size of the nano-phase inclusion is below 30nm, and such small size formed is likely due to high graft reaction activity and grafting degree. The SEM micrograph of PANI-*g*-PolyCuPc-*g*-PU sample in Figure 28(b) exhibited a homogeneous structure even under the magnification of 20K, and no inclusion phases can be observed, even when oligomer content is increased to 35%. In comparison, as shown in Figure 28(c), the simple blend containing oligomer content, 30wt%, the aggregates with several μm sizes were observed in the polymer matrix. These results reveal that chemically bonding of the oligomers to the backbones of the polymer matrix can improve the compatibility of the oligomers and matrix, while aggregation of oligomers can be very hard to prevent in the physical blends. Furthermore, improvement of the

dispersibility of oligomers in polymer matrix makes the system self-organize the nanocomposites possessing oligomer nano-phase within the fully functionalized polymers. It is known that phthalocyanine as well as oligoaniline has a strong tendency to form stack assemblies due to its planar shape and aromatic nature. In this oligomer graft polyurethanes, oligomer attached on the main chain can act as a nucleation center, which further induces the growth of oligomer clusters. Since the pendent oligomer is distributed separately along the polymer backbone and especially distributed in the hard segment of segmented polyurethane. The size of aggregates is restricted by the accessibility of adjacent oligomer molecules in the polymer networks. Thus, oligomer nanophases are in situ formed in the polymer matrix. Referring to the SEM micrographs showing details of the fractured structures of the blends and nano-polymers, although the pullout of the oligomer microparticles occurs from the polymer matrix in simple blend as shown in Figure 10(c), the polymer matrix still remains tightly associated with the oligomer nanophases in the full-functionalized nano-polymer in Figure 10(b). During the shape deformation of the polymers under external fields, immobilization of nanophases and polymer backbones via chemically bonding reduces greatly the relative motion and further aggregation of the nanophases within the polymer matrix, which improve the material reliability and breakdown field.

In summary, we have developed novel fully functionalized high-dielectric-constant nano-phase polymers in which the high dielectric constant PolyCuPC as well as conductive oligomeric anilines are chemically grafted to the backbone of polyurethane. Due to the high degree of the grafting, the oligomer phase size is significantly reduced to below 30 nm, as well as more uniformly distributed in the matrix compared with blends. One consequence of such a nano-phase polymer is the significantly increased interface effect, which through the exchange coupling results in an enhanced dielectric response, confirming a recent theoretical prediction. Consequently, these self-organized nano-phase polymers exhibit a high dielectric constant, reduced low dielectric loss, and an improved breakdwown field and reliability, all of which are highly desirable for high dielectric constant materials for actuator and dielectric applications. More importantly, the high dielectric constant nano-phase polymers exhibit one order of magnitude reduction or more in the applied field in achieving high strain and elastic energy density in comparison with single phase EAPs with similar strain level and elastic energy density. Specifically, these nano-phase polymers offer a high dielectric constant (a dielectric constant near 1,000 at 20 Hz), a longitudinal strain of more than -14% induced under a much reduced field, 23 V/μm, with an elastic energy density of higher than 1 J/cm^3. The elastic modulus is as high as 100MPa, and a transverse strain is 7% under the same field.